Determining the molecular mehanisms regulating lysosome damage and repair pathways

Božić, Mihaela

University of Zagreb
Faculty of Science
Division of Biology

Mihaela Božić

Determining the molecular mechanisms regulating lysosome damage and repair pathways

Graduation Thesis

Zagreb, 2018.

University of Zagreb
Faculty of Science
Division of Biology

Mihaela Božić

Determining the molecular mechanisms regulating lysosome damage and repair pathways

Graduation Thesis

Zagreb, 2018.

This thesis, written at the University of Dundee – School of Life Sciences, Dundee, United Kingdom, under the supervision of Dr. David McEwan, has been submitted for evaluation to the Division of Biology, Faculty of Science, University of Zagreb, for the title of Master of Molecular Biology.

Acknowledgements

Firstly, I would like to thank dr. David McEwan for taking me into his lab, twice, answering a million, and more, of my questions, and teaching me all of the skills I'm proud to know to today.
I would like to thank everyone in the McEwan lab for their help and good company, especially Nina Dawe for help with endless pipetting, and Nicola Goodman for the best proofreading job ever.
Thanks to the Dundee Phenotypic screening facility for processing all of the screening plates.
Zahvaljujem doc.dr. Ingi Marijanović za vođenje mog diplomskog rada na Prirodoslovno-matematičkom fakultetu.

Zahvaljujem cijeloj svojoj bližoj obitelji, posebice svojim najdražim, i jedinim, teti i tetku, Andreji i Samu za najveću pomoć i potporu kroz sve što sam prolazila.
Veliko hvala mom Josipu što je uz mene sve ove godine, za strpljivo gledanje svih mojih rezultata i što je najbolja osoba koju poznajem.
Za kraj, najveća hvala mojoj mami, što je najbolja mama koju mogu poželjeti, što je najbolja prijateljica i prva na koju sam uvijek mogla računati.

BASIC DOCUMENTATION CARD

University of Zagreb

Faculty of Science

Division of Biology

Graduation Thesis

DETERMINING THE MOLECULAR MECHANISMS REGULATING LYSOSOME DAMAGE AND REPAIR PATHWAYS

Mihaela Božić

Horvatovac 102a, 10000 Zagreb, Croatia

Lysosomes are organelles surrounded by a single lipid layer, encapsulating hydrolytic enzymes, and serve as cell's primary catabolic compartments. Lysosome membranes are easily damaged by the intake of lyososomotropic agents such as L-Leucyl-L-Leucine methyl ester (LLOMe). This event can be recognized by recruitment of Galectin3 to the damaged membranes. Damaged lysosomes can be further repaired, or cleared by autophagy. Autophagic degradation of the lysosomes themselves is termed lysophagy. Little is known of how the cell senses that damage, how it is repaired, or how LLOMe mediated lysosome damage impacts autophagy flux. By overexpressing fluorophore tagged Galectin3 damaged lysosomes can be counted and LLOMe influence characterized. siRNA knock down of specific genes will result in higher number of Galectin3 signal when silenced genes are involved in lysosome damage recognition and repair/clearance. Here, we provide 7 genes identified as possible mediators of the lysosomal biogenesis pathways that can serve as base for future studies and further validation. Identifying those pathways could serve a therapeutic potential in tumours with high levels of cathepsins, inflammations, infections, and neurodegenerative diseases. We also characterize influence of LLOMe intake on autophagy flux, being simultaneously a potent autophagy inducer, and inhibitor of autophagy progression by autophagosome-lysosome fusion.

(45 pages, 8 figures, 4 tables, 104 references, original in: English)

Thesis is deposited in: Central biological library

Keywords: autophagy, lysophagy, LMP, LLOMe, Galectin3, siRNA

Supervisor: David McEwan, PhD

Reviewers: David McEwan, PhD

Inga Marijanović, PhD, Asst. Prof.

Maria Špoljar, PhD, Assoc. Prof.

Nada Oršolić, PhD, Prof.

Thesis accepted: 19/9/2018

TEMELJNA DOKUMENTACIJSKA KARTICA

Sveučilište u Zagrebu

Prirodoslovno-matematički fakultet

Biološki odsjek

Diplomski rad

ODREĐIVANJE MOLEKULARNIH MEHANIZAMA U REGULACIJI OŠTEĆENJA I POPRAVKA LIZOSOMA

Mihaela Božić

Horvatovac 102a, 10000 Zagreb, Croatia

Lizosomi su organeli omeđeni jednostukom membranom, sadržavaju hidrolitičke enzime i služe kao primarni katabolički organeli eukariotskih stanica. Lizosomi su vrlo podložni oštećenju pri ulasku lizozomotropnih spojeva, kao što je detergent L-leucil-L-leucin metil ester (LLOMe), u stanicu. Takav događaj može se prepoznati prema regrutaciji proteina Galektin3 na oštećenu membranu lizosoma. Oštećeni lizosomi posljedično bivaju popravljeni ili razgrađeni putem autofagije. Do sada je vrlo malo poznat poces prepoznavanja i popravlja takva oštećenja, te kako oštećenje lizosoma izazvano detergentom LLOMe utječe na process autofagije. Ekspresijom fuzijskog proteina GFP-Galektin3 oštećeni lizosoma mogu se vizualizirati i izbrojati. Utišavanje pojedinih gena pomoću siRNA rezultira u povećanom broju Galektin3 u stanici ako su ti geni uključeni u prepoznavanje oštećenih lizosoma ili njihov popravak/degradaciju. U ovom radu predlažemo 7 gena prepoznatih kao medijatore puta biogeneze lizosoma koji mogu poslužiti kao baza za daljnja istraživanja i detaljnu karakterizaciju staničnih signalnih puteva. Potpuno razumijevanje mehanizma prepoznavanja oštećenih lizosoma i njihovog popravka može poslužiti pri identifikaciji terapeutske mete kod tumora s visokom razinom katepsina, upala, infekcija i neurodegenerativnih bolesti. Također pružamo uvid u utjecaj LLOMe na proces autofagije i označavamo LLOMe kao snažan induktor autofagije, te istovremeno inhibitor napretka progresije autofagije pri koraku fuzije autofagosoma s lizosomom.

(45 stranice, 8 slika, 4 tablica, 104 literaturnih navoda, jezik izvornika: engleski)

Rad je pohranjen u: Središnja biološka knjižnica

Ključne riječi: autofagija, lizofagija, LMP, LLOMe, galectin3, siRNA

Mentor: dr. sc. David McEwan

Ocjenitelji: dr. sc. David McEwan

doc. dr. sc. Inga Marijanović

izv. prof. dr. sc. Maria Špoljar

prof. dr. sc. Nada Oršolić

Rad prihvaćen: 19/9/2018.

TABLE OF CONTENTS

LIST OF ABREVATIONS

ALR – Autophagic lysosome reformation
AMBRA1 - Activating molecule in Beclin1-regulated autophagy
AMPK - 5′ adenosine monophosphate-activated protein kinase
BSA – Bovine serum albumin
CASA – Chaperone-mediated selective autophagy
CMA – Chaperone-mediated autophagy
CRD – Carbohydrate recognition domain
CTSC – Cathepsin C
DAPI - 4′,6-diamidino-2-phenylindole
ddH_2O – Double distilled water
DMEM – Dulbecco's Modified Eagle Medium
DMSO – Dimethyl sulfoxide
EDTA - Ethylenediaminetetraacetic acid
ER – Endoplasmic reticulum
ERGIC - ER-Golgi intermediate compartment
EtOH – Ethanol
FBS – Fetal bovine serum
GABARAP - GABA-A receptor-associated protein
Gal-3 – Galectin-3
GFP – Green Fluorescent Protein
HIF1 – Hypoxia induced factor 1
HOPS - Homotypic fusion and protein sorting
HRP – Horseradish peroxidase
HSC – Heat shock cognate
HSP – Heat shock protein
JNK1 - c-Jun N-terminal protein kinase 1
LAMP1 – lysosomal-associated membrane protein 1
LAMP2 – lysosomal-associated membrane protein 2
LIR – LC3 interacting region
LLOMe - L-Leucyl-L-Leucine methyl ester
LMP – Lysosomal membrane permeabilization
MAP1LC3 - Microtubule-associated protein 1 light chain 3

MOMP - Mitochondrial outer membrane permeabilization

mTORC1 – mammalian target of rapamycin complex 1

NaCl – Sodium chloride

PAS - Phagophore assembly site

PE - Phosphatidylethanolamine

PFA – Paraformaldehyde

PI - Phosphoinositide

PI3K – Phosphoinositide 3-kinase

PI3P – Phosphatidylinositol 3-phosphate

Plekhm1 – Pleckstrin homology-domain containing family member 1

REDD1 - Regulated in development and DNA damage response 1

RHEB - Ras homolog enriched in brain

ROS – Reactive oxygen species

RT – Room temperature

SDS – Sodium dodecyl sulfate

SDS-PAGE - SDS polyacrylamide gel electrophoresis

SNAREs – Soluble N-ethylmaleimide-sensitive fusion attachment protein receptors

TBS – Tris-buffered saline

TBST – Tris-buffered saline-Tween 20

TCEP - Tris(2-carboxyethyl)-phosphine

TCL – Total cell lysis

Ub – Ubiquitin

ULK1 – Unc-51-like kinase 1

VCP - Valosin-containing protein

WT – Wild type

1. Introduction

1.1. Autophagy

Autophagy, derived from the Greek "self" and "eating", was first described in 1960's while studying the function of lysosomes. It was noticed that large intracellular structures, such as mitochondria are degraded within the lysosome (de Duve and Wattiaux, 1966). The understanding of autophagy as a novel cellular pathway started with the observation of glucagon-induced formation of the autophagic vesicles, and changes in lysosomal morphology during induction (Deter and De Duve, 1967). From there, the importance of autophagy in homeostasis of the cell has emerged, with studies in this field exploding in the last decade.

Autophagy is a cellular degradative process occurring primarily as a response to nutrient stress. It serves to provide nutrients in times of starvation through recycling of the macromolecules via the lysosome. Autophagy plays a major housekeeping role in removing of misfolded proteins, protein aggregates, clearance of damaged organelles, and pathogen elimination (Glick, Barth and Macleod, 2010). Although autophagy was initially considered to be non-selective, recent advancements have shown evidence of selectivity of cargo, including organelles, pathogens and protein aggregates (Svenning and Johansen, 2013). Three main types of autophagy exist: chaperone-mediated autophagy (CMA), microautophagy, and macroautophagy (Figure 1.), all of which have been recognized by different means of cargo intake and delivery to the main degradation centre of the cell – the lysosome (Hamacher-Brady, 2012). This thesis will focus specifically on the process of macroautophagy.

1.1.1. Macroautophagy

Macroautophagy (henceforth "autophagy") is the most extensively studied type, and differs from others by the formation of a double membrane vesicle intermediate called the autophagosome. Autophagy consists of several sequential steps, which involve induction, autophagosome formation, autophagosome-lysosome fusion, and degradation (Pyo *et al.,* 2012). In yeast, the biogenesis of autophagosomes commences at the phagophore assembly site (PAS), a protein-vesicle ultrastructure that is organized by the Atg1 complex (human ULK1/2) (Köfinger *et al.*, 2015), and Atg9 facilitates membrane flow to the PAS (He *et al.*, 2008). Mammalian autophagy has been proposed to commence either at the ER-mitochondrial junction or the ER-Golgi intermediate compartment (ERGIC) (Stanley *et al.*, 2014). Upon phagophore closure, autophagosomes can briefly exists as amphisomes by fusion with the endosome, prior

to degradation (Sanchez-Wandelmer and Reggiori, 2013). Otherwise they directly fuse with the lysosome, followed by maturation to an autolysosome (Sasaki *et al.*, 2017) where the cargo is degraded.

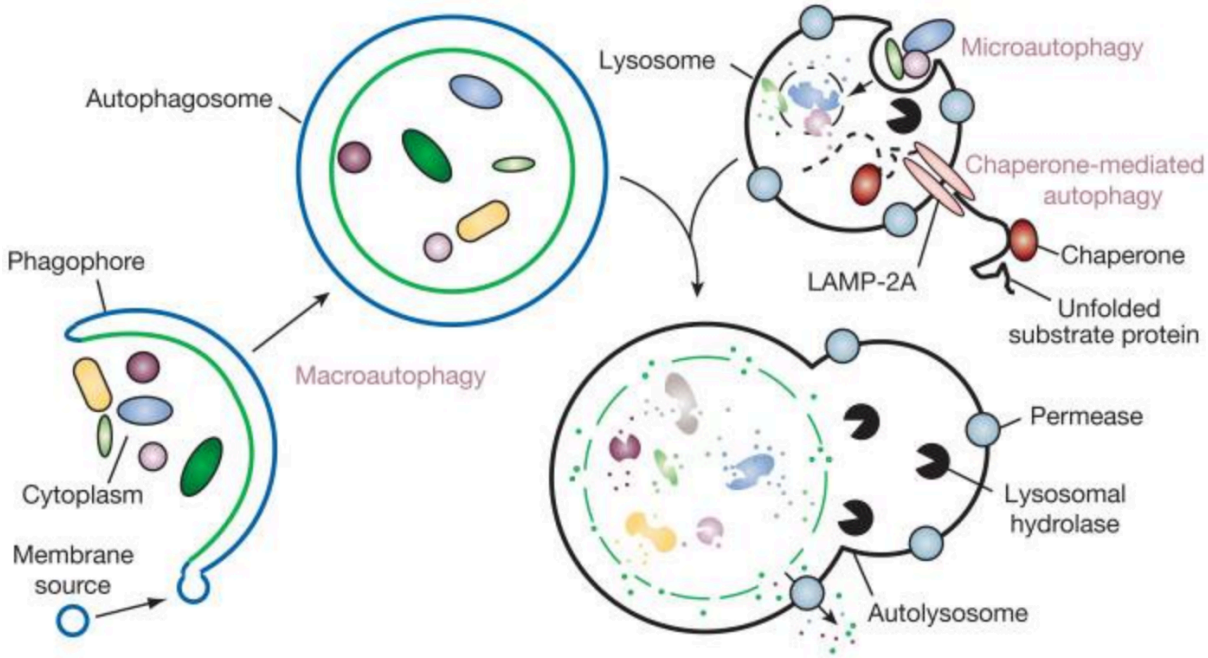

Figure 1. Overview of three main types of autophagy and their differences (Mizushima *et al.*, 2008).

1.1.2. Signalling cascades controlling autophagy initiation

In many cell lines, autophagy is strongly induced by glucose starvation, amino-acid deprivation and stress conditions, such as hypoxia and reactive oxygen species (ROS) (Figure 2.). Key energy sensors regulate the induction of autophagy under these conditions in order to provide sufficient energy and building blocks for survival. 5′ adenosine monophosphate-activated protein kinase (AMPK) is one of those sensors, and it is activated under starvation conditions by mitochondria-generated ROS (Li et al, 2013). AMPK promotes autophagy by directly activating the ULK1 (Unc-51-like kinase 1), homologue of yeast Atg1 initiator protein, through phosphorylation of Ser 317 and Ser 777.

Contrary to this, one of the key autophagy inhibitors is the mammalian target of rapamycin (mTOR), a central cell-growth regulator that integrates growth factor and nutrient

signals. Under conditions of nutrient sufficiency, high mTOR activity prevents ULK1 activation by phosphorylating ULK1 Ser 757, disrupting the interaction between ULK1 and AMPK (Kim *et al*., 2011). mTOR belongs to the PI3K-related protein kinase family and controls cell growth, in part by regulating p70 S6 kinase alpha and eukaryotic initiation factor 4E binding protein 1 (4EBP1) (Hara *et al*., 2002). It can assemble as two complexes; mTORC1, interacting with the Raptor subunit, and mTORC2, interacting with the Rictor subunit. Both complexes have distinct downstream effects, mTORC1 being rapamycin-sensitive (Hara et al., 2002). mTORC2 being rapamycin-insensitive (Kim *et al*., 2012). In times of deprivation, AMPK play its role by directly phosphorylating Raptor, and inhibiting mTORC1 *(Gwinn et al*., 2008).

MAP kinase p38 and ERK, mediators of inflammatory signals, respond to environmental stress, and are thought to have an effect on autophagy. p38 inhibits autophagy and promotes inflammatory responses by phosphorylating ULK1 (He *et al*., 2018). ERK, positioned downstream of AMPK regulates autophagy through Beclin1. Activation of ERK by AMPK upon autophagy stimuli disassembles mTORC1 and mTORC2 complexes, eventually causing an increase in Beclin1 activity (Wang *et al.*, 2009; Tong et al., 2015).

1.1.3. Formation, elongation and closure of autophagosomes

Autophagic machinery is involved in each of the steps mentioned previously that lead to lysosomal degradation of encapsulated cargo (Figure 2). Functional studies in yeast Saccharomyces cerevisiae led to discovery of a series of conserved genes involved in the process of autophagy. The unified nomenclature was proposed ATG ("AuTophaGy related") gene, and Atg for corresponding protein (Klionsky et al., 2003). Currently, over 30 ATG genes have been discovered to be involved in autophagosome formation and biogenesis (Kang et al., 2018). Yeast ATG genes were only the beginning in the characterization of mammalian autophagic machinery genes, which are organized in similar hierarchical manner (Suzuki et al., 2007; Mizushima et al., 2011). In mammals, the majority of Atg proteins are found to have multiple isoforms which corresponds to the higher complexity of the organism involved (Zientara-Rytter and Subramani, 2018).

Mammalian phagophore formation starts at the ER-mitochondrial junction or the ERGIC, and yeast at the PAS, involving autophagy in the *de novo* formation of membrane

structures. Nucleation of the isolation membrane starts with Beclin1 and its association with the class III PI3K core complex generating PI3P (Funderburk et al., 2010). Phagophore membranes are recognized as Atg9-containing vesicles which originate from the Golgi apparatus, and are required for early autophagosome formation (Yamamoto, 2012).

Atg1, a yeast homolog of human ULK1, is an essential component of the initiation machinery (Ganley, 2009). It is responsible for phosphorylation of Atg9, and consequently the recruitment of machinery that promotes elongation and closure of the autophagosome (Galluzzi *et al*., 2017). Furthermore, Atg2 associates to autophagosomal membranes through lipid binding. Its interaction with Atg9 is responsible for Atg18 recruitment. Assembly of the Atg9-Atg2-Atg18 complex is important to establish phagophore-ER contact sites (Gómez-Sánchez *et al*., 2018).

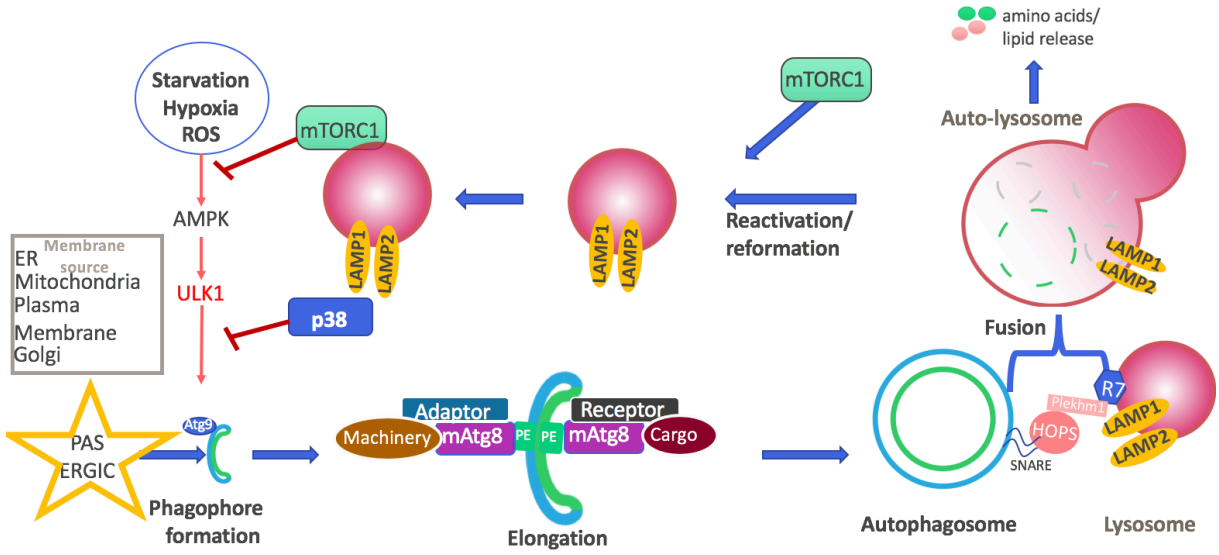

Figure 2. Autophagy signalling leading to induction of autophagy, formation of an autophagosome, membrane elongation, and final step of fusion with the lysosome.

Ubiquitin-like conjugation systems is involved in further development of an autophagosome, before fusion with the lysosome. Atg7 is an E1-like (ubiquitin activating enzyme) protein, which, together with Atg5, conjugates Atg12 depending on ATP hydrolysis, and Atg10 being an E2-like (ubiquitin—conjugating) protein (Mizushima *et al.*, 1998). Atg16 interacts with Atg12-Atg5, forming the Atg12/Atg5/Atg16 complex essential for

autophagosome membrane elongation, and works as an E3-like (ubiquitin ligase) complex (Mizushima *et al.*, 1999). Together with Atg3 (E2-like protein) and Atg7, the complex works to conjugate phosphatidylethanolamine (PE) to mAtg8 homologues and facilitate their integration in the autophagosomal membrane (Figure 3.) (Galluzzi *et al.*, 2017). In mammalian cells, there are six Atg8 orthologues that are divided into two main families; the microtubule-associated protein 1 light chain 3 (MAP1LC3s; LC3A, LC3B and LC3C) and γ-aminobutyric acid receptor-associated proteins (GABARAP, GABARAP-L1, and GABARAP-L2/GATE16) (Nguyen *et al.*, 2016). The lipidated forms of these proteins, which are anchored to the autophagosomal membrane via PE and promote cargo recruitment, largely accumulate in the cell when autophagic flux is impaired, corresponding to large number of non-degraded autophagosomes (Martens, 2016). For that reason, these proteins are widely used as autophagic markers. LC3 is predominantly conjugated to the luminal surface of the autophagosome membrane, and GABARAP at the cytoplasm-facing side, suggesting its diversity in function. Autophagy receptors interact directly with mATG8s on the inner autophagosomal membrane, providing a link between the autophagosomal membrane and cargo, and autophagy adaptor proteins interact with mATG8 proteins on the convex autophagosomal membrane surface to regulate autophagosome formation (Figure 2**.**) (Rogov *et al.*, 2017). Throughout autophagosome maturation, LC3 is cleaved by Atg4 cysteine proteases, generating LC3-I, which is then conjugated to PE by Atg7 and Atg3 (Figure 3.). Lipidated LC3, termed LC3-II, is then associated with newly forming autophagosome membranes. Upon fusion with the lysosome, LC3-II on the outer membrane of autophagosome is converted back into LC3-I by Atg4 (Hamacher-Brady, 2012). GABARAPs are thought to be involved in the final closure of the autophagosome (Martens, 2016).

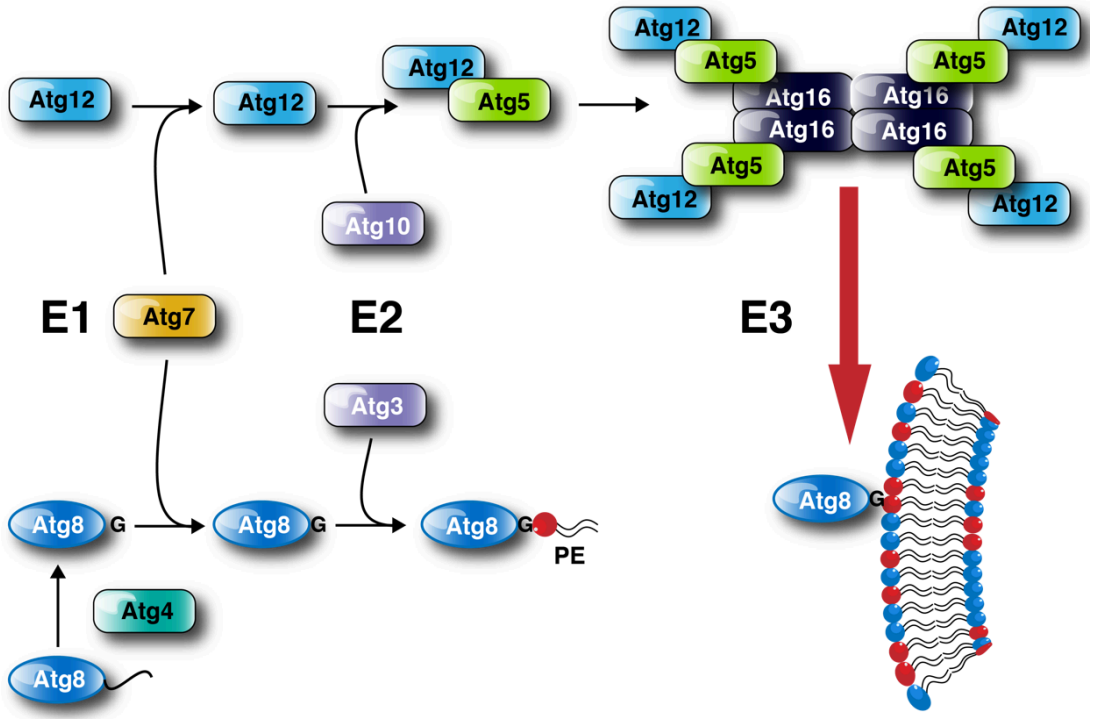

Figure 3. Ubiquitin-like conjugation system driving autophagosomal membrane expansion through Atg8 conjugation to PE.

1.1.4. Autophagosome-lysosome fusion and degradation

After the autophagosome is finally closed it is ready to fuse with the lysosome and its cargo degraded, providing nutrients for the cell in times of degradation. Fusion events depend on the GTPase Rab7 and the homotypic fusion and protein sorting (HOPS) complex. Furthermore, adaptor protein Pleckstrin homology domain containing protein family member 1 (PLEKHM1) directly interacts with this HOPS complex (McEwan *et al.*, 2015) and contains a GABARAP interaction motif (Rogov *et al.*, 2017) mediating its binding to autophagosomal membranes. Rab7 is a key component in autophagosome maturation, interacting with the lysosomal membrane proteins LAMP1 and LAMP2, and aids the fusion process (Jäger *et al.*, 2004). The tethering HOPS complex binds to late endosomes and lysosomes through Rab7 and directly recruits soluble NSF attachment protein receptors (SNAREs) that work towards membranes fusion (Chen and Klionsky, 2011). SNAREs involved in this process include VAMP7, VAMP8, VTI1B, SNAP29 and STX17 (McEwan and Dikic, 2015).

The final step, the degradation of the enclosed cargo, is achieved by acidification of the autolysosome by v-ATPases and the disintegration of the inner autophagosomal membrane,

supported by Atg4, mediating the removal of mAtg8s from the membrane surface. Upon completion, several lysosomes can emerge from an autolysosome, in the step termed 'autophagic lysosome reformation' (ALR), thus restoring the lysosome viability (Galluzzi *et al.*, 2017).

1.1.5. Selective Autophagy

Autophagy is mostly recognized for its non-specific and bulk degradation of parts of the cytoplasm which is crucial for cell homeostasis and survival during stress. Autophagy has become more and more recognized as being selective for its cargo; targeting organelles, thus, regulating organelle number and integrity (Anding and Baehrecke, 2017), involved in selective clearance of intercellular pathogens such as bacteria (Sorbara and Girardin, 2015), and viruses (Sumpter *et al.*, 2016), and the removal of toxic protein aggregates (Svenning and Johansen, 2013b). Enormous diversity in key players mediating this process has emerged, with major contribution to autophagy receptors and adaptors that have high variety and specificity. Autophagy receptors interact with the autophagic substrates and mATG8s on the luminal autophagosomal membrane. They serve to link the cargo to the growing autophagosomal membrane, and allow the recognition of specific cargo (Stolz *et al.,* 2014). Many of the receptors have ubiquitin (Ub)-binding domains that allows the recruitment of the cargo to the crescent membrane. Ubiquitination plays a role in selective autophagy as well, serving as a tag for misfolded proteins, or damaged organelles (Kirkin *et al.*, 2009). These receptors are mostly specific for a certain type of selective autophagy. For example, NDP52, OPTN, TAX1BP1 and p62 have a predominant role in the clearance of damaged mitochondria, termed mitophagy (Narendra *et al.*, 2010), NBR1 and p62/SQSTM1 are involved in the degradation of peroxisomes ("pexophagy") (Deosaran *et al.*, 2013), and the clearance of protein aggregates (Clausen *et al.*, 2010). FAM134B in mammals, or Atg40 in yeast, target parts of the ER in the process called ER-phagy (Mochida *et al.*, 2015), while NDP52 and Optineurin mediate the clearance of cytosolic bacteria escaped from the vacuole (Sorbara and Girardin, 2015). Even more specific cargo receptors have emerged in the last few years showing glycogen clearance (Jiang *et al.,* 2011), zymogen granules (Grasso *et al.*, 2011), and iron-binding ferritin complexes (Ryu *et al.*, 2018) to use specific degradation pathways.

Autophagy adaptors, on the other hand, bind mATG8s on the convex site of the autophagosomal membrane and help recruit the autophagy machinery. They are important for

the formation (ULK1/2 complex), elongation and transport of the autophagosome as well as its fusion (PLEKHM1-HOPS complex) with the lysosome (Pankiv, 2007). Although different in function, both autophagy adaptors and receptors share a motif ([W/F]-[V/I]-X2-V) that allows them to interact with GABARAPs – and is a recently modified version of the original LC3 interaction region (LIR; WxxL) motif (Noda, Ohsumi and Inagaki, 2010)

1.2. Lysosomes – composition and function

Lysosomes are single membrane enclosed organelles containing an array of enzymes capable of breaking down all types of biological polymers. They function as the main digestive system of a cell, degrading both external material and components of the cell itself. Lysosomes vary in size and shape as a result of the different material to be degraded. Lysosomes contain around 50 degradative enzymes that can hydrolyse proteins, DNA, RNA polysaccharides, and lipids. All of the lysosomal enzymes are acid hydrolases, which are active around pH 5 that is maintained within lysosomes. To maintain their acidity, must actively concentrate H^+ ions by a proton pump in the lysosomal membrane. That process is largely dependent of ATP. The lysosomal membrane contains a large number of proteins including lysosome-associated membrane protein 1 (LAMP1), LAMP2, LYNUS, CIC7, and TCP1/2 (Saftig and Klumperman, 2009). To prevent the degradation of its own membrane, their membrane luminal side is covered in glycocalyx, a polysaccharide-based coating (Settembre *et al.*, 2013). Beside their apparent function in protein homeostasis and metabolism, the lysosome is also crucial for other systems. Secretion of lysosomal components plays an important role in cytotoxic T cell function, bone resorption, parasite defence and plasma membrane repair (Saftig and Klumperman, 2009). Moreover, the lysosome plays an important role in cell signalling, growth, Ca^{2+} storage, autophagy and protein biosynthesis as mTORC1 activity was reported to localize to the lysosomal membrane (Settembre *et al.*, 2013). Mutations of lysosomal proteins or any pathways involving lysosomal biogenesis and function are the cause of many diseases affecting kidneys, livers, muscles, pancreases, bones and neuro-cognitive functions (Saftig and Klumperman, 2009).

1.2.1. Lysosomal membrane permeabilization (LMP)

Lysosomes are known to be highly susceptible to damage. Silica and aluminium salt crystals activate NALP3-formed inflammasomes, causing phagocytosis of crystals as well as lysosomal damage and rupture (Hornung *et al.*, 2008). Certain detergents have lysosomotropic properties,

and found its use in lysosomal membrane targeting in many studies. Upon entering the cell, they work through permeabilizing the lysosomal membrane, eventually causing its rupture, and release of lysosome content to the cytosol (Villamil Giraldo *et al.*, 2014). L-leucyl-L-leucine methyl ester (LLOMe) is the most common of those, and is often used to induce LMP *in vitro* (Thiele and Lipsky, 1990). β-amyloid protein aggregates were found to disrupt membranes containing acidic phospholipids, and cause lysosomal rupture *in vivo* (McLaurin and Chakrabartty, 1996). Cathepsin C (CTSC), also known as dipeptidyl peptidase I (DPP-I), is a lysosomal protease enzyme from the peptidase C1 family. In cells, CTSC is responsible for biotransformation of lyososomotropic agents such as LLOMe. LLOMe is cell permeable, but inactive until it is transformed by CTSC within the lysosome and induces LMP (Thiele and Lipsky, 1990; Jacobson *et al.*, 2013). The autophagy-lysosome pathway is shown to be regulated by valosin-containing protein (VCP), a key player in protein quality control (Meyer *et al.,* 2012). VCP is essential for maturation of ubiquitin-containing autophagosomes, and its deregulation impairs normal lysosome biogenesis, thus inhibiting fusion with the lysosome (Thurston *et al.*, 2012; Ju *et al.*, 2009).

Damage of lysosomes is linked to pathological states such as Parkinson's disease, infection, and inflammatory disease (Dehay *et al.*, 2010). It is thought to be a potentially catastrophic event for a cell, releasing lysosomal lumen content including cathepsins (Palermo and Joyce, 2008) and H^+ ions into the cytosol, causing DNA damage or a decrease in lysosomal degradation ability (Boya and Kroemer, 2008). The release of lysosomal proteases is able to cause digestion of additional hydrolases such as caspases, causing a downstream cascade reaction of Bid activation by cleavage with lysosomal cathepsins B and D. This induces mitochondrial outer membrane permeabilization (MOMP), release of cytochrome c, finally resulting in apoptotic (Type I) cell death (Boya and Kroemer, 2008). Furthermore, lysosomal damage reduces the catabolic capacity of the lysosome which may lead to acidification of the cytosol ultimately leading to necrosis (Type III cell death) (de Duve and Wattiaux, 1966).

Lysosomal quality control is based on the identification of small soluble proteins that bind β-galactosidase on glycoproteins called galectins. Galectins are an evolutionary conserved family of ß-galactose-binding proteins that comprises 15 members. Containing a carbohydrate recognition domain (CRD), galectins are found in the cytoplasm, nucleus and extracellular space where they perform a variety of functions. While the extracellular pool is important for cell migration, endocytosis and adhesion, galectins within the cell assist in cell growth,

apoptosis and immunity (Thurston *et al.*, 2012). Galectins are generally synthetized in the cytosol and displayed in the lumen, patrol the cytoplasm and recognize compromised membranes by detecting components of the glycocalyx (Kumar *et al.*, 2017).

Galectin3 (Gal3) has a single CRD and a disordered N-Terminal site for oligomerization. It can be found extracellularly, in the nucleus, or in the cytoplasm. Gal3, similar to Gal8, is recruited to endolysosomes, lysosomes and phagosomes in response to bacterial-induced vesicle damage (Thurston *et al.*, 2012). N-linked glycosylation is essential for cell surface binding and recruitment to lysosomes. Galectin-3 is found to be specifically recruited to the surface of damaged lysosomes. For this reason, fluorophore-tagged Gal3 is often used as a reporter for lysosomal damage (Paz *et al.*, 2010).

1.2.2. Lysophagy

Damaged lysosomes are targeted for repair or eventually cleared by autophagy through the autophagosome, eventually restoring low pH and lysosomal degradation capacity (Maejima *et al.*, 2013). Selective autophagy of the lysosomes is called lysophagy. Similar to other forms of selective autophagy, lysophagy is initiated by ubiquitination of the damaged lysosomes and recruitment of the autophagic machinery to the affected vesicles. Upon LMP, TRIM16 (a member of TRIM family E3 ubiquitin ligases) interacts with Galectin-3, and mediates mobilization of ULK1, Beclin1 and Atg16L. Interaction with Galectin-3 serves for recognition of the damaged lysosome, while ubiquitination of ULK1 and Beclin1 (and, consequently, the ubiquitination of lysosome) leads to downstream recruitment of LC3 and p62 (Chauhan *et al.*, 2016). Furthermore, two SNARE proteins, VAMP3 and VAMP7, and five lysosomal proteins, LAMP1, LAMP2, GNS, PSAP, and TMEM192 can also be found ubiquitinated upon lysosomal damage (Yoshida *et al.*, 2017). How this process of recognition and repair/removal intersects with the components of other trafficking pathways, such as the endocytic, is unclear.

1.3. Aim of the study

Fluorophore (GFP) tagged Galectin3 enables direct visualization of LLOMe-mediated lysosomes damage. siRNA knock down of potential genes involved in lysosome homeostasis, recognition of lysosome damage, or regulating lysosome repair and clearance will result in altered (increased or decreased) number of Galectin3 puncta compared to siRNA control

conditions. Using this knowledge, we aim to identify several candidate genes to serve as starting point for describing those cellular processes. For that reason, high content screening of siRNA library is performed.

Using immunofluorescence experiments and Western blot analysis this study aims to:

1. Characterise the formation and localization of Galectin3 puncta in the cell
2. Identify the effect lyososomotropic agents have on induction and progression of the autophagy pathway
3. Develop a strict protocol for automated siRNA screening to be used for future screening analysis

Answers provided by this study will be used to conduct further screening analysis using different set of genes, and genes identified by the initial screening will be taken into further validation and creating targeted stable knock out cell lines.

2. Materials and methods

2.1. Cell culture

U2OS – human osteosarcoma cell line was used to conduct all of the experiments described further in the text (Table 1.). U2OS is an adherent cell line, easily maintained in culture (Table 2.), they are readily transfected, and have a good cytoplasm to nucleus ratio, which makes them suitable for the confocal microscopy based studies. U2OS stably transfected with fusion protein GFP-Galectin3 carrying plasmid (pEGFP-hGal3) is a reporter cell line, used to visualise lysosomal damage when, upon treatment with lyososomotropic agents such as LLOMe, Galectin3 is recruited to the damaged membranes.

Table 1. Cell lines used to conduct the experiments.

U2OS WT (human osteosarcoma)	American Type Culture Collection (ATCC)
U2OS GFP-Gal3 (human osteosarcoma stably expressing GFP-Galectin-3)	pEGFP-hGal3 was a gift from Tamotsu Yoshimori (Addgene plasmid #73080) (Maejima *et al.*, 2013). Stable expression was established by transfection and selection in G418 selective medium (see Table 3). Single cell clones were sorted with thanks to the FACS department (University of Dundee) previously in our lab.

The cell lines used were cultured and maintained in medium conditions as described in table 3. Both were regularly passaged every 3-4 days, and kept at 37 °C and at 5 % CO_2.

Table 2. Cell culture media conditions.

Name	**Components**	**Use**
Full Medium (FM)	DMEM (Gibco™ Dulbecco's Modified Eagle Medium, Thermo Fisher Scientific), 10 % FCS (Gibco™ Thermo Fisher Scientific), 1% Penicillin-Streptomycin (Gibco™ Thermo Fisher Scientific), 1 mM Sodium Pyruvate (Lonza Group)	U2OS WT cell line maintenance
G418 Selective medium (G418S)	DMEM, 10 % FCS, 1 % Penicillin-Streptomycin, 1 mM Sodium Pyruvate, 800 µg/ml G418 solution (Formedium™)	U2OS GFP-Gal3 cell line maintenance

antibiotic - Free medium (AF)	DMEM, 10 % FCS, 1 mM Sodium Pyruvate	U2OS GFP-Gal3 cell line maintenance post-siRNA transfection

2.2. Transient Transfection

U2OS WT cells were used in immunofluorescence experiments, and for this purpose were transiently transfected with a GFP-expressing plasmid (pcDNA5 FRT/TO-GFP, Addgene plasmid #19444). Cells were grown to 70-90 % confluency, trypsinized, counted, and plated on circular cover glass in a 12-well dish at a density of $1*10^5$ cells/well. The plates were incubated at 37°C, 5% CO_2, for approx. 16 h. Cells were then treated with 1:10 OptiMEM (Thermo Fisher Scientific) containing TurboFect Transfection Reagent (Thermo Fisher Scientific), and pcDNA5 FRT/TO-GFP (1:500, 1 μg, respectively) in FM, then incubated for an additional 24 h (37 °C, 5 % CO_2).

2.3. LLOMe-induced Lysosome Damage and Recovery

To induce lysosome membrane damage cells were treated with 1 mM LLOMe (Sigma-Aldrich) and left for 1 h at 37 °C, 5 % CO_2. As a control group, cells were treated with LLOMe solvent (1 % ethanol) for 1 h. For recovery, sample group cells treated with 1 mM LLOMe for 1 h were gently washed in 1 x PBS, and left in fresh FM at 37 °C, 5 % CO_2 for 8 h (siRNA screening samples) or 16 h (immunofluorescence and Western blot samples). Additionally, cells were treated with 200 nM Bafilomycin A1 (BafA1, Santa Cruz Biotechnology Inc.) during the recovery time for Western blot analysis of the U2OS GFP-Gal3 cells.

2.4. Antibodies and preparation

Antibodies used in all of the experiments of this study are presented in Table 3.

For Western blot analysis, primary antibodies were prepared in 5% bovine serum albumin (BSA) in PBS, with the exception of p62 antibody which is prepared in 1% milk in PBS. Secondary antibodies for that purpose were prepared in 5% milk diluted in TBS-T buffer

(20 mM Tris, 150 mM NaCl, 0,1 % TWEEN 20 pH 7.5 – 7.6). For immunofluorescence experiments, primary and secondary antibodies were both prepared in 5% BSA in PBS with 0,1% Saponin (Sigma-Aldrich).

Table 3. Datasheet showing antibodies used in all of the experiments.

Use	Antigen/Conjugate	Clone	Dilution	Source
Immunoblotting				
Primary Antibodies	p-ULK1	Polyclonal	1/1000	Cell Signalling Technology
	p-Plekhm1	Polyclonal	1/1000	Produced-In-House
	Plekhm1	Polyclonal	1/1000	Sigma-Aldrich
	LAMP-1	H4A3	1/1000	Developmental Studies Hybridoma Bank
	LAMP-2	H4B4	1/1000	Developmental Studies Hybridoma Bank
	p62	5F2	1/1000	Medical & Biological Laboratories
	pERK1/2	D13.14.4E	1/1000	Cell Signalling Technology
	ERK1/2	137F5	1/1000	Cell Signalling Technology
	GABARAP	Polyclonal	1/1000	AbGent
	LC3	5F10	1/1000	nanoTools
	Vinculin	hVIN-1	1/10000	Sigma-Aldrich
Secondary Antibodies	Anti-rabbit IgG, HRP-linked Antibody	-	1/1000	Cell Signalling Technology
	Anti-mouse IgG, HRP-linked Antibody	-	1/1000	Cell Signalling Technology
Immunofluorescence				
Primary Antibodies	LAMP-2	H4B4	1/500	Developmental Studies Hybridoma Bank
	LC3-B	Polyclonal	1/500	Medical & Biological Laboratories
Secondary Antibodies	Alexa Fluor-555 anti-mouse IgG	-	1/300	Invitrogen – Life Technologies
	Atto 647-N anti-rabbit IgG	-	1/300	Sigma-Aldrich

2.5. Immunofluorescence Staining

For immunofluorescence experiments both U2OS WT and U2OS GFP-Gal3 cells were used. When 70-90 % confluent, cells were set on round glass cover slips at a density of $1*10^5$ cells/well, and incubated for an additional 16 h. Following this, both cell lines were treated with 1mM LLOMe to induce lysosome damage, and U2OS GFP-Gal3 cells were additionally recovered in FM conditions for another 8 h. Cells were fixed in 4% PFA (Santa Cruz Biotechnology Inc.) in 1 x PBS solution for 10 minutes at RT, washed twice in 1 x PBS, and stored in 1 x PBS, at 4°C, protected from light until ready for staining.

For staining the cells were permeabilized by washing in 0.1 % Saponin (Sigma-Aldrich) in 1 x PBS, twice for 10 seconds. They were then incubated in primary antibody solutions plus 5 pM DAPI for 1 h at RT in a humidified dark chamber. The cells were then washed 2 x 10 seconds in 0.1 % Saponin in 1 x PBS, and incubated for 45 min in secondary antibody solution as before. The cover slips were washed 2 x 10 seconds in 0.1 % Saponin 1 x PBS, 10 seconds in 1 x PBS, then 10 seconds in ddH_2O. Cover slips were mounted using Mowiol mounting medium on microscope slides, and left to air dry at RT, protected from light.

Images were taken using LSM 710 Confocal Laser Scanning Microscope (Zeiss) at 63x magnification, using 518 F immersion oil (Thermo Fisher Scientific). GFP was excited using an argon laser at 488 nm for 0.6 – 0.9 seconds. Atto 647 - N and AlexaFluor 555 were excited with a helium-neon laser at 543 and 635 nm, respectively, for 0.5 – 0.6 seconds. Images were later sorted and analysed using Fiji (ImageJ, version 1.51w).

2.6. Immunoblotting

For immunoblotting experiments, U2OS GFP-Gal3 cells were used at 70-90 % confluency, set at a density of $5*10^5$ cells/well in 6 well dishes. Cells were then treated as described with 1% solvent (Et-OH), 1mM LLOMe for 1h, 1 mM LLOMe followed with recovery in FM for 16 h, and 1 h LLOMe followed by recovery in FM containing 200 nM BafA1 for 16 h. Following treatment, the cells were lysed on ice in 100 µL TCL buffer (50 mM Tris, 1 mM MgCl2, 150 mM NaCl, 1 % SDS, pH 7.5) topped with 1 x Protease inhibitor (Roche), 1 x Phosphatase inhibitor (Roche) and 50 U Benzonase (Novagen). All samples were mixed with 2 x SDS-PAGE Loading Sample Buffer (1 M Tris-HCL (pH 6,8), 10 % SDS, 5 % Glycerol, 0,5 M TCEP, 1 % Bromphenol Blue), and boiled at 95 °C for 10 minutes. Samples were loaded and proteins were separated by electrophoresis at 200 V for 40 min using a 4-12 % Bis-Tris gel (Invitrogen) in 1 x MES SDS Running Buffer (Invitrogen). Proteins were transferred on methanol-activated PVDF membrane for 90 min at 200 mA using 1 x Transfer Buffer (50 mM Tris, 40 mM Gycine, 1:5 methanol).

Membranes were blocked in 5 % BSA 1 x PBS for 1 h, at RT. Membranes were then incubated with primary antibody solution overnight at 4 °C. Next day membranes were washed 3 x 5 minutes in 1x TBS-T Buffer (20 mM Tris, 150 mM NaCl, 0,1 % TWEEN 20 pH 7.5 –

7.6), incubated with secondary antibody solution (HRP-conjugated) for 1 h, at RT, followed by additional washing in TBS-T. For chemiluminescence, ECL (GE Healthcare Life Sciences) or ECL Plus (ThermoFisher Scientific) substrate solutions were used, and the membranes were imaged using Azure c600 Fluorescence and Chemiluminescence Imaging System Azure Biosystems) with an exposure time of 1-5 minutes at high resolution. Images were later sorted and analysed using Fiji (ImageJ, version 1.51w).

2.7. High content screening of siRNA library

siRNA libraries (GE Dharmacon) were prepared with 4 siRNA sequences per well; a total of 487 genes (in 6 primary plates), which included 139 human membrane trafficking genes (siGENOME™ siRNA Library – Human Membrane Trafficking G-005505, GE Dharmacon), 256 human phosphatases (siGENOME™ siRNA Library – Human Phosphatase G-003705, GE Dharmacon), and 92 custom genes including autophagy-related and control genes (iGENOME™ siRNA Library - LP_26422 – G-CUSTOM-254242, GE Dharmacon). From the primary siRNA library, working plates were prepared by resuspending dry siRNA library plates in the 5x siRNA Resuspension Buffer (Sigma-Aldrich) to a 2 μM stock. These were further diluted into working plates to a 100 nM concentration. Control Non-Target siRNA (siGENOME™ Control Pool – Non-Targeting #2, GE Dharmacon) was also diluted to 100 nM in siRNA Resuspension Buffer, and distributed to wells A1, A2 and A3 of each plate. The rest of the empty wells were filled with resuspension buffer only and used as additional controls. 100 nM working plates were stored at -20 °C, and further used to prepare each of the 4 repeats. U2OS GFP-Gal3 cells were grown to a 70-90 % confluency, harvested, and diluted to $6*10^4$ – $7.5*10^4$ cells/mL in AF medium (see Table 3.) to prepare for reverse transfection. 3 plates for each siRNA were set corresponding each condition (Control (EtOH), LLOMe, or Recovery). siRNAs were distributed in plates in final 1 ρmol concentration, mixed with 1:100 Lipofectamine® RNAiMAX Reagent (Invitrogen – Life Technologies) in OptiMem (Thermo Fisher Scientific) and incubated for 20 minutes at RT to form an siRNA-Lipofectamine-OptiMem complex. Cells were then added to the plates at a final concentration of 4000 – 6000 cells/well, and incubated for 48 h at 37 °C, 5 % CO_2. After 48 h, each plate was treated with 1% solvent (Et-OH), 1 mM LLOMe for 1 h, or 1 mM LLOMe for 1 h followed by recovery in FM condition for 8 h. Upon finished treatment cells were fixed with warm 4 % PFA for 10 min at RT, washed twice with 1 x PBS, and stored in 1 x PBS at 4 °C.

Prior to screening, cells were additionally stained with 1:15000 HSC CellMask (Thermo Fisher Scientific) and 1:4000 DAPI (5 nM) in 10 % Saponin PBS solution for 30 minutes at RT. Plates were washed 3 x with 1 x PBS, and stored in 1 x PBS at 4°C, protected from light.

Images were acquired using the IN Cell Analyzer 2200 Imaging System (GE Healtchare Life Sciences) using 0.4, 0.7 and 1.9 seconds exposure time for DAPI, HSC CellMask and GFP, respectively. CellProfiler (version 2.1.0.), an open source cell image analysis software, was then used to process and analyse the images. Cells were filtered for dead cells based on DAPI and HSC CellMask, and GFP channel puncta were counted.

2.8. Statistics

Data generated by CellProfiler (version 2.1.0.) was analysed using Excel and GraphPad Prism 6 (version 7.0d.) Puncta per cell was determined by counting the number of filtered nuclei and GFP-Gal3 puncta per field, and averaged for each field image per well (6 images per well). These numbers were further averaged using the 4 experimental repeats, and data was divided per condition as: Control (EtOH), LLOMe, Recovery 8 h, and Non-Target siRNA as a negative control. Standard deviation was calculated for each condition, and averaged for each repeat. As proposed, the 2-3 times fold-change of the aberration of standard deviation should be applied (Jung and Behrends, 2017), so to calculate the cut off score, % of puncta per cell (mean S.D/mean Non-target control), were then multiplied by the standard fold-change of 1.49. The number generated was used to create top (mean Non-target * 100% + stand. %puncta/cell) and bottom (mean Non-target – (mean Non-target * stand. %puncta/cell) cut off score. Results were then represented graphically using GraphPad prism 6 (version 7.0d.) and Excel, and potential "hits" were characterised as value above/bellow the cut off score. To further significate the scores, the original siRNA screen images were taken into account and compared to a number of puncta in wells containing negative and positive control siRNAs. The negative control siRNA used was the CTSC (cathepsin c) gene, a gene responsible for metabolising LLOMe into its active form (Thiele and Lipsky, 1990), whose silencing consequently stops Galectin-3 recruitment to the lysosomal membrane. As a positive control, autophagic machinery genes were used; upon knockdown, these result in similar numbers of GFP-Gal3 puncta in recovery as in the LLOMe treatment group (Maejima *et al.*, 2013). A final list of "hits" was characterized using genes involved in lysosomal homeostasis (higher number of GFP-Gal3 puncta in control

condition (EtOH) compared to Non-target control), genes involved in lysosomal damage recognition (reduced number of GFP-Gal3 puncta in treatment condition (LLOMe), and genes involved in removal/repair of damaged lysosomes (higher number of GFP-Gal3 puncta after recovery).

3. Results

3.1. LLOMe treatment forms Gal-3 puncta on the lysosomal membrane

The model used to conduct this study was first tested to confirm GFP-Gal3 puncta formation upon treatment with LLOMe. Two related immunofluorescence experiments were performed for that purpose. First experiment was carried out using our model cell line U2OS stably expressing GFP-Gal3. Cells were prepared as control – treated with solvent 1% EtOH, LLOMe treatment for 1h, and Recovery in FM conditions after initial LLOMe treatment for 16h. After initial treatment GFP-Gal3 was seen to form into puncta in the cell (Figure 4. A), while recovery resulted in significant clearance of GFP puncta from the cell, and return to the condition seen in the control cells treated with solvent, 1% EtOH. Second experiment was carried out using the U2OS WT cells transiently transfected with pcDNA5 fr/to GFP carrying plasmid, treated with LLOMe for 1h. GFP transfected into the U2OS WT cells was seen dispersed throughout the entire cell, and stayed unchanged after LLOMe treatment. GFP alone was not seen forming into puncta in response to treatment (Figure 4. B).

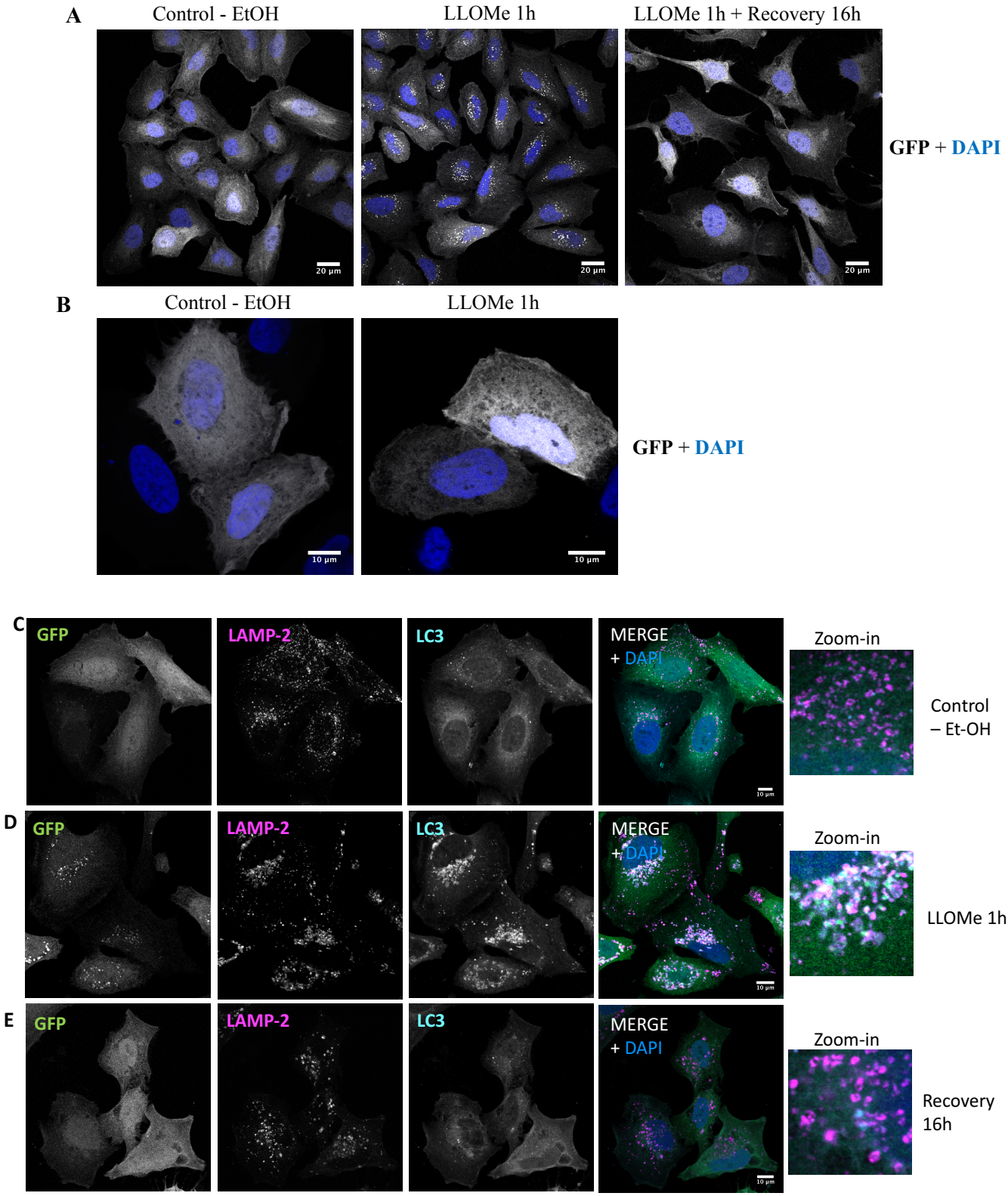

Figure 4. Formation of the GFP-Gal3 puncta and co-localization with autophagosome maker protein LC3, and lysosome marker protein LAMP2.
Immunofluorescent analysis of the GFP-Gal3 puncta formation in the U2OS GFP-Gal3 cell line treated as LLOMe (1 mM) and Recovery condition (A), and treated control U2OS WT cell line transiently transfected with GFP carrying plasmid (B), GFP cahnnel is shown in grayscale. U2OS GFP-Gal3 (green) cells stained for autophagy markers; LC3 (turquoise) and LAMP2

(magenta) under three conditions: control – treated with solvent 1% EtOH (C), induced LMP with LLOMe (1 mM) treatment 1h (D), and recovery 16h in FM after initial LLOMe treatment (D). All of the cells were co-stained with DAPI (blue).

U2OS GFP-Gal3 model cells therefore, responded to lysosomal damage in the form of recruitment of GFP-Gal3 on the membrane of the damaged lysosomes, which allows a visual of that event. Observed puncta, and their location within the cell was further characterised by co-staining GFP-Gal3 cells for autophagic markers. For that purpose, immunofluorescence assay was prepared using LC3 and LAMP2 antibodies, markers for autophagosomes, and lysosomes respectively. In control cells, treated with 1% solvent (EtOH), no GFP-Gal3 puncta was seen, while a great number of LAMP2 positive vesicles was observes, corresponding to the normal number of lysosomes found in the cell at any given time. Few of the LC3 positive vesicles were seen, co-localized with the LAMP2 vesicles, which marks a basal levels of autophagy process in the cell (Figure 4. C). When cells were treated with LLOMe, GFP-Gal3 puncta is observed forming and co-localizing with the LAMP2 positive vesicles, proving the localization of the GFP-Gal3 to the damaged lysosome membranes. A large increase in the levels of LC3 was observed co-localizing with LAMP2, marking LLOMe as a potent autophagy inductor. LC3 was observed in the same amount as LAMP2, which was increased compared to the number of lysosomes in control cells, suggesting LLOMe to block further progress of induced autophagy, by blocking degradation of the autophagosome encapsulated cargo (Figure 4. D). After recovery GFP-Gal3 was cleared from the cells, and only a few of LC3 positive vesicles were observed. Autophagy process was finished, and damaged lysosomes were repaired, or cleared by autophagy. To confirm the degradation of damaged lysosome, number of LAMP2 positive vesicles was also observed in lower levels than it was in the control cells (Figure 4. E).

3.2. LLOMe simultaneously activates autophagy by inhibition of mTOR, but inhibits autophagy progression by inhibiting lysosomal degradation

To further test the effects LLOMe has on the cells, and on the autophagy flux, a Western blot experiment was preformed using the U2OS GFP-Gal3 cells. Cells were treated as control, 1h with LLOMe to induce lysosomal damage, recovery in FM for 16h, and recovery in FM with added Bafilomycin A1 for 16h. BafA1 is responsible for inhibition of both lysosomal V-ATPase and therefore autophagosome-lysosome fusion (Mauvezin and Neufeld, 2015). Cells were probed with antibodies involved in autophagy, inflammation and metabolism. As shown

in Figure 5., and in confirmation of immunofluorescence data (Figure 4.) LLOMe proved to be a potent autophagic flux inducer. That is seen by observing a large amount of p-ULK1 levels in cells treated with LLOMe. ULK1 is phosphorylated by AMPK, followed by the release of autophagic core complex, and induction of autophagosome formation. pULK1 levels are reduced in both Recovery, after clearance of damaged vesicles, and Recovery with BafA1 which corresponds to the reduced levels of autophagy under these conditions. Accumulation of lipid ated forms of LC3 and GABARAP were observed with LLOMe treatment suggesting a block in autophagy progression which corresponds to the BafA1 treated sample. High levels of p62/SQSTM1 autophagy receptor were also observed in LLOMe treatment and Recovery with BafA1. Accumulation of LC3, GABARAP and p62 is often a marker for impaired autophagy flux corresponding to accumulation of damaged vesicles, which are not cleared by autophagosome-lysosome fusion. Unpublished data from our lab suggests dual regulation of Plekhm1, via autophagy (mTOR), and through MAPK pathway. From those data, it is clear that mTORC1 directly phosphorylates Plekhm1, and that phosphorylation inhibits the function of Plekhm1, and consequently autophagy flux. Levels of p-Plekhm1 are greatly increased upon treatment with LLOMe (Figure 5.) which additionally proves block in autophagy progression due to the damage made by LLOMe on the lysosome membranes. Total Plekhm1 was used as a control for approximating levels of p-Plekhm1. Accumulation of damaged lysosome is evident from the increased levels of lysosome markers LAMP1 and LAMP2. Activation of ERK by AMPK upon autophagy stimuli was seen in the increased levels of p-ERK1/2 with LLOMe treatment, which was abolished after blocking autophagy progress with BafA1. Total ERK1/2 was used to approximate the levels of phosphorylated ERK1/2. Levels of GFP-Gal3 remain constant, and high in all conditions, as it is overexpressed in the U2OS GFP-Gal3 cells. GFP only was observed degrading from the Gal3 in Recovery and Recovery + BafA1, and appears as a smear on the blot. Vinculin was used as loading control for all the other probes.

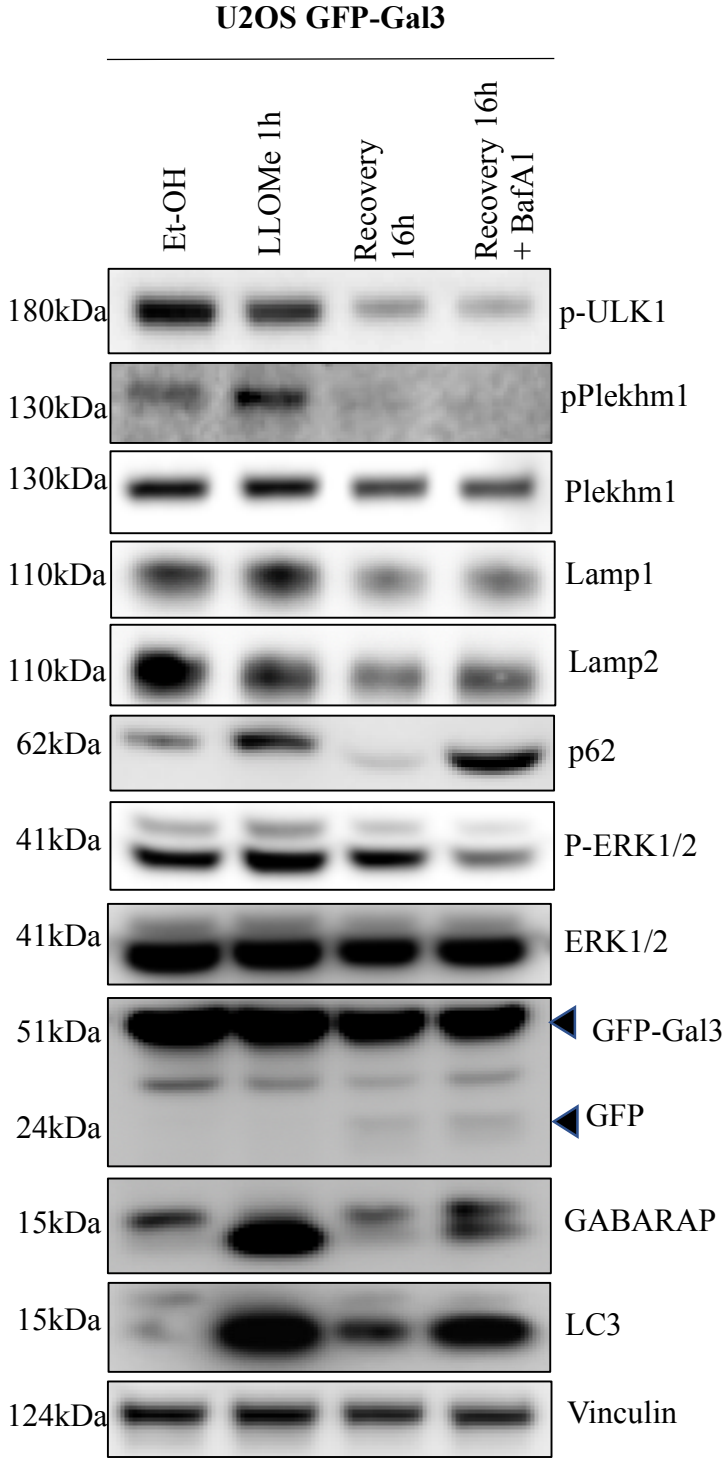

Figure 5. LLOMe simultaneously stimulates autophagy flux, but inhibits the progression of autophagy by blocking the final step of cargo degradation. U2OS GFP-Gal3 cells were treated as control (1% solvent – EtOH), LLOMe (1mM) induction of LMP for 1h, Recovery for 16h in FM after initial LLOMe treatment, and Recovery with Bafilomycin A1 (200 nM). Western blot images of total cell lysates probed for proteins involved in autophagy, inflammation and metabolism are shown. Vinculin was used as loading control.

3.3. siRNA library screen produces a list of genes involved in lysosomal biogenesis

U2OS GFP-Gal3 cells were plated, one plate per condition (Control, LLOMe, and Recovery), reverse transfected with siRNA library, treated, and prepared for imaging by co-staining with DAPI and HSC CellMask. Genes targeted by corresponding siRNA were divided into two parts, here described as Membrane trafficking/G-custom, containing genes involved in membrane trafficking and custom siRNA plates targeting autophagy related genes, and Phosphatases. Scores recorded for each well containing certain siRNA corresponding to number of GFP-Gal3 puncta per cell were represented graphically by Excell, and compared to the Non-target control siRNA score. Calculated top and bottom cut off score in each condition is represented by a horizontal line (Supplementary Information, Image S1. A-F.) For the purpose of better view, the results were filtered, showing only genes identified as "hits", meaning having their average puncta per cell scores above or below the cut off line (Figure 6. A-F**.**). Cut off scores are shown in red, while top and bottom cut off lines are shown with orange and green line respectively. Out of 487 genes targeted by siRNAs, 231 genes were described as membrane trafficking and custom genes. 39 of these were identified as potential "hits" in the cells treated as Control with 1% solvent (EtOH) (Figure 6. A), 39 in the cells treated with LLOMe (Figure 6. B), and 19 in the Recovery condition (Figure 6. C). LLOMe in not converted to its active form when CTSC gene is silenced by siRNA, therefore CTSC gene was used as negative control. In the wells containing CTSC GFP-Gal3 was observed to form only few puncta resulting in its low puncta per cell score in both LLOMe and Recovery (Figure 6. B, C**.**), VCP was used as positive control. Its deregulation results in abnormal lysosomal biogenesis and inability to clear the autophagic cargo by fusion with the lysosome. VCP silencing results in high number of GFP-Gal3 puncta in cell remaining after recovery (Figure 6. C), and therefore was used as positive control.

Even more potential "hits" were identified with the screening for 257 cell's phosphatases, resulting in 107 genes identified as potential "hits" in Control – EtOH (Figure 6. D), 55 in the LLOMe treatment (Figure 6. E), and 22 genes discovered in the Recovery condition (Figure 6. F).

A

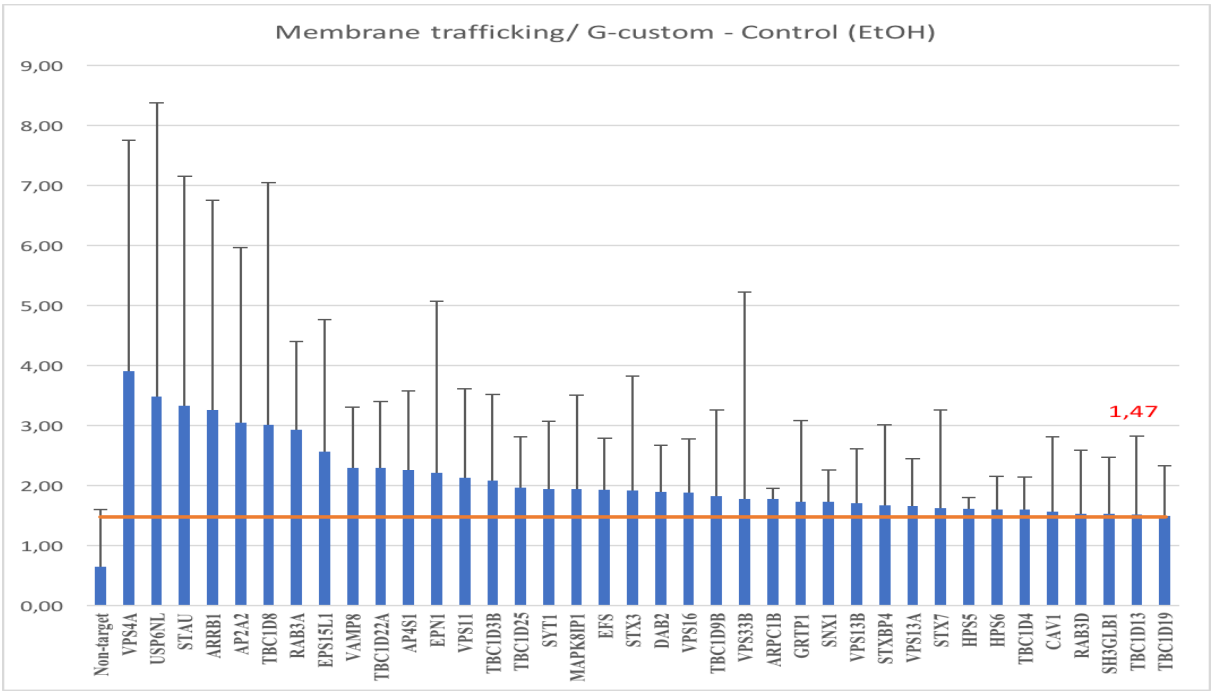
Membrane trafficking/ G-custom - Control (EtOH)
9,00
8,00
7,00
6,00
5,00
4,00
3,00
2,00
1,00
0,00
1,47
Non-target
VPS4A
USP6NL
STAU
ARRB1
AP2A2
TBC1D8
RAB3A
EPS15L1
VAMP8
TBC1D22A
AP4S1
EPN1
VPS11
TBC1D3B
TBC1D25
SYT1
MAPK8IP1
EFS
STX3
DAB2
VPS16
TBC1D9B
VPS33B
ARPC1B
GRTP1
SNX1
VPS13B
STXBP4
VPS13A
STX7
HPS5
HPS6
TBC1D4
CAV1
RAB3D
SH3GLB1
TBC1D13
TBC1D19

B

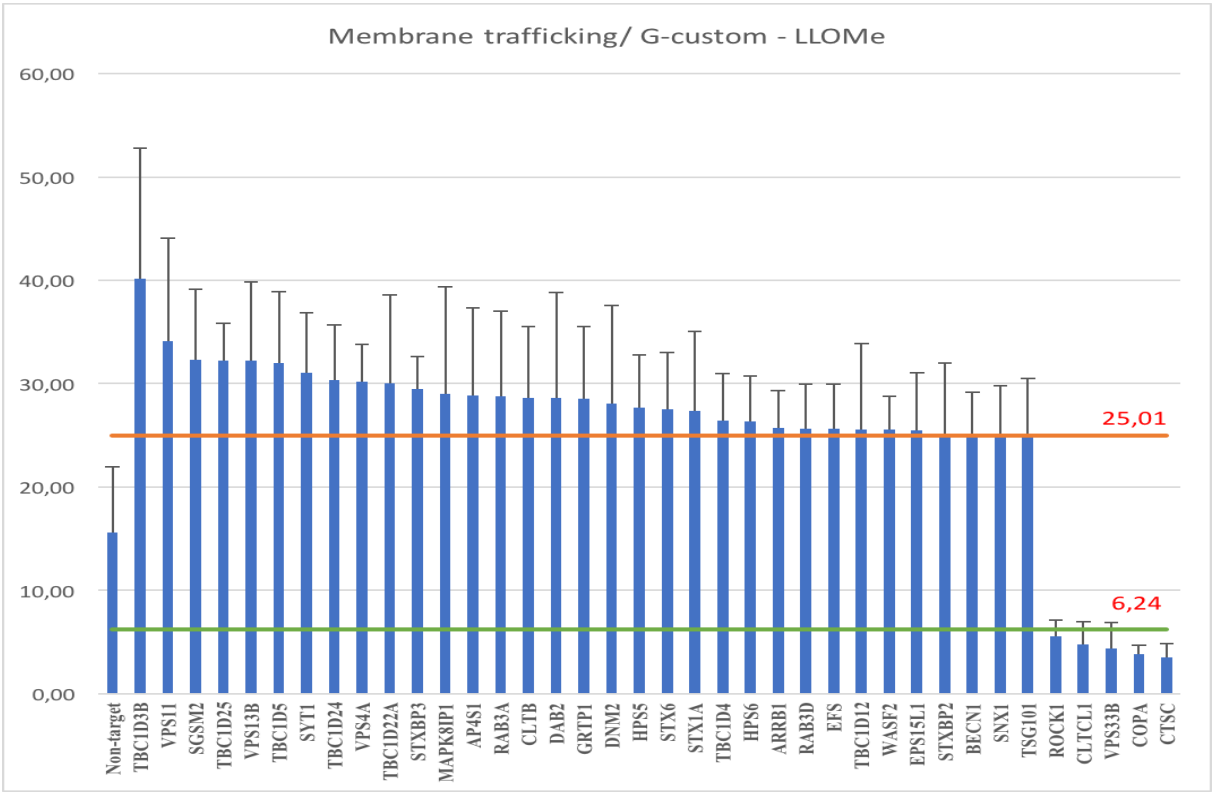
Membrane trafficking/ G-custom - LLOMe
60,00
50,00
40,00
30,00
20,00
10,00
0,00
25,01
6,24
Non-target
TBC1D3B
VPS11
SGSM2
TBC1D25
VPS13B
TBC1D5
SYT1
TBC1D24
VPS4A
TBC1D22A
STXBP3
MAPK8IP1
AP4S1
RAB3A
CLTB
DAB2
GRTP1
DNM2
HPS5
STX6
STX1A
TBC1D4
HPS6
ARRB1
RAB3D
EFS
TBC1D12
WASF2
EPS15L1
STXBP2
BECN1
SNX1
TSG101
ROCK1
CLTCL1
VPS33B
COPA
CTSC

C

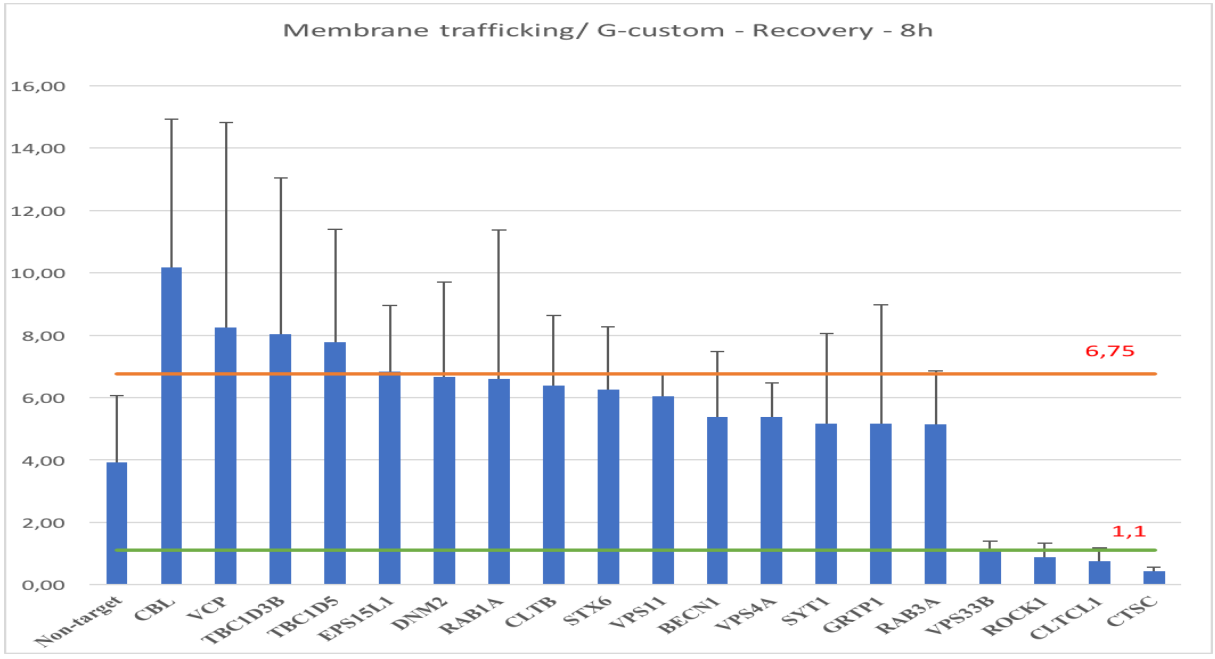
Membrane trafficking/ G-custom - Recovery - 8h
16,00
14,00
12,00
10,00
8,00
6,00
4,00
2,00
0,00
6,75
1,1
Non-target
CBL
VCP
TBC1D3B
TBC1D5
EPS15L1
DNM2
RAB1A
CLTB
STX6
VPS11
BECN1
VPS4A
SYT1
GRTP1
RAB3A
VPS33B
ROCK1
CLTCL1
CTSC

D

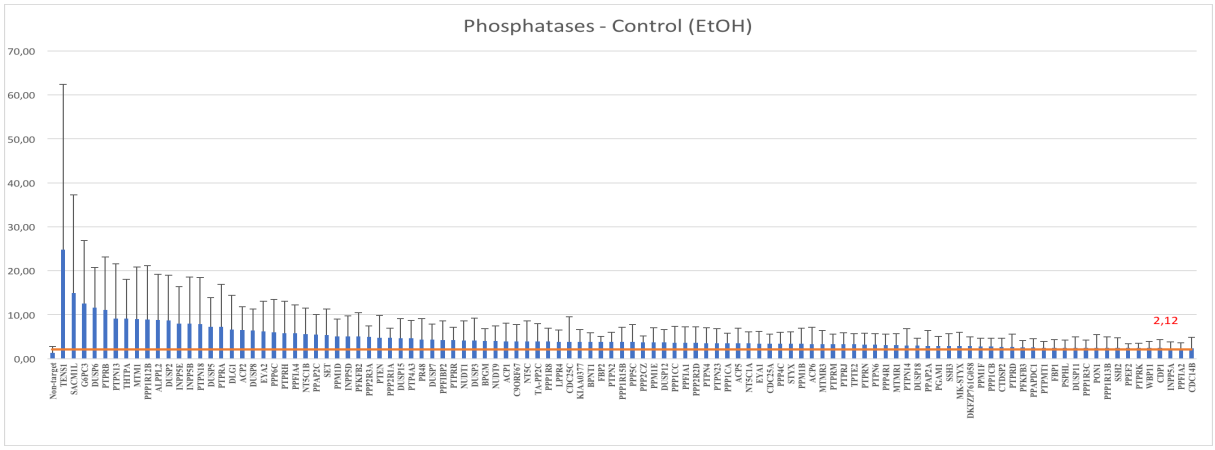
Phosphatases - Control (EtOH)
70,00
60,00
50,00
40,00
30,00
20,00
10,00
0,00
2,12

E

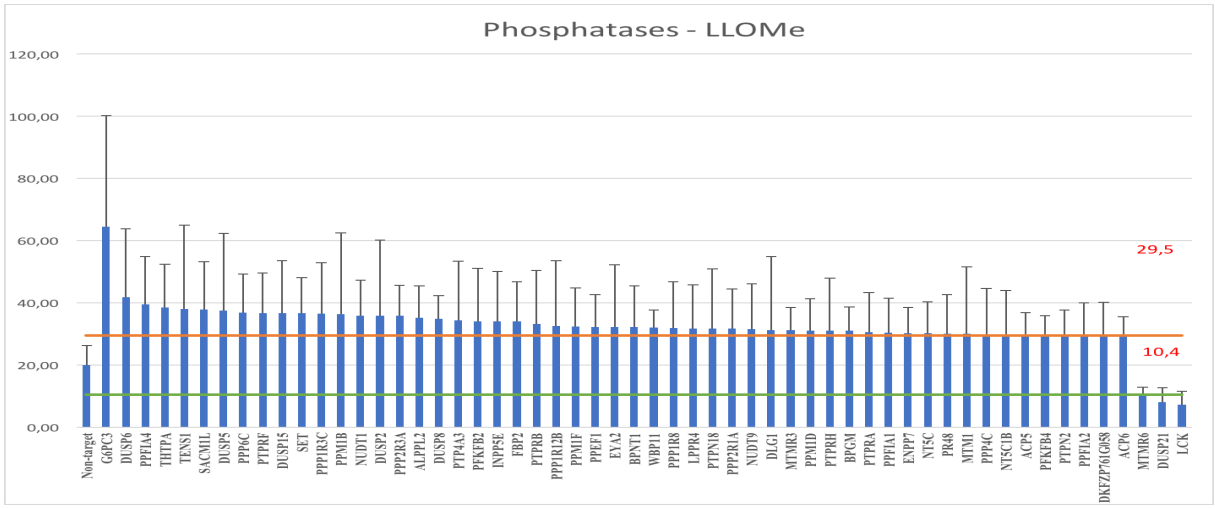
Phosphatases - LLOMe
120,00
100,00
80,00
60,00
40,00
20,00
0,00
29,5
10,4
Non-target
G6PC3
DUSP6
PPEF1A4
THTPA
TENS1
SACM1L
DUSP5
PPP6C
PTPRF
DUSP15
SET
PPP1R3C
PPM1B
NUDT1
DUSP2
PPP2R3A
ALPPL2
DUSP8
PTP4A3
PFKFB2
INPP5E
FBP2
PTPRB
PPP1R12B
PPM1F
PPEF1
EYA2
BPNT1
WIPI1
PPP1R8
LPPR4
PTPN18
PPP2R1A
NUDT9
DLG1
MTMR3
PPM1D
PTPRH
BPGM
PTPRA
PPEF1A1
ENPP7
NT5C
PR40
MTM1
PPP4C
NT5C1B
ACP5
PFKFB4
PTPN2
PPEF1A2
DKFZP761G058
ACP6
MTMR6
DUSP21
LCK

F

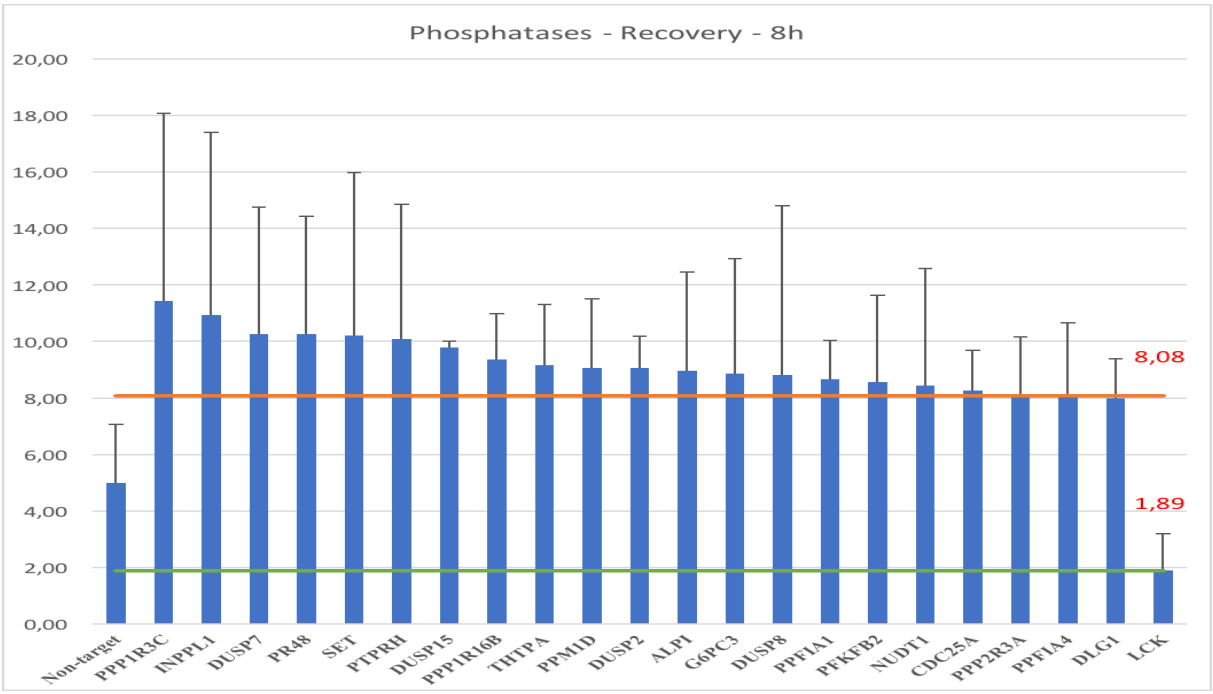

Figure 6. Potential "hits" identified with siRNA library screening for the genes involved in lysosomal biogenesis.
Data generated by the screening analysis measured as number of GFP-Gal3 puncta per cell, has been statistically analysed, and top (orange line) and bottom (green line) cut off scores calculated (shown in red). Data is further represented as the average puncta per cell, per gene silenced by corresponding siRNA, in descending order. Shown on the figure are genes identified as potential "hits" meaning, presenting their average puncta/cell score above of bellow the cut off lines. A-C are shown Membrane trafficking/custom genes in Control-EtOH, LLOMe and Recovery, respectively. D-F are shown cellular Phosphatases in the same order of conditions.

Genes represented are identified as "hits", meaning that their average GFP-Gal3 puncta per cell identified a score significantly higher or lower that the cut-off score calculated by the Non-target control (Figure 6.). These were sorted by descending order from the original charts including the complete list of genes contained in the siRNA library (Figure S1. A-F).

Membrane trafficking and custom genes identified as "hits" were further validated by taking original images, and data of puncta per cell, per well produced through screening, and genes with outstanding images and values were excluded from the list of "hits" producing more targeted and valid list of genes potentially included in lysosomal biogenesis (Table 4.). Genes were separated by the condition marking genes included in lysosome homeostasis (Control – EtOH), genes involved in recognition of lysosome membrane damage (LLOMe), and genes involved in repair and/or clearance of damaged lysosomes (Recovery). Genes identified as potential "hits" in all three conditions are marked in red.

Table 4. Genes identified to be potential "hits", involved in lysosomal biogenesis pathways.

Membrane trafficking/Custom genes		
Control - EtOH	**LLOMe 1h**	**Recovery 8h**
CAV1	AP4S1	BECN1
DAB2	BECN1	CBL
GRTP1	CLTB	CLTB
RAB3A	CLTCL1	CLTCL1
SNX1	COPA	CTSC
STX7	CTSC	DNM2
STXBP4	DAB2	EPS15L1
SYT1	DNM2	GRTP1
TBC1D22A	EPS15L1	RAB1A
TBC1D3B	GRTP1	RAB3A
TBC1D4	HPS5	ROCK1
TBC1D9B	HPS6	STX6
USP6NL	MAPK8IP1	SYT1
VPS11	RAB3A	TBC1D3B
VPS13B	ROCK1	VCP
VPS16	SGSM2	VPS11
VPS33B	STX1A	VPS33B
VPS4A	STX6	VPS4A
	STXBP2	
	SYT1	
	TBC1D12	
	TBC1D22A	
	TBC1D3B	
	VPS11	
	VPS13B	
	VPS33B	
	VPS4A	

Genes identified by the high content siRNA screening to potentially be involved in lysosome biogenesis through further validation of "hits" generated with statistical analysis of siRNA screening data. Genes identified under Control – EtOH are thought to be involved in general lysosome homeostasis, genes under LLOMe 1h condition in lysosome damage recognition, and genes under Recovery 8h condition in lysosome repair/clearance pathway. Genes identified as "hits" in all three conditions are shown in red.

Original images that are taken into account for validation of identified genes are shown in Figure 7, 8 (A-H**)**. By treating siRNA silenced positive control gene, VCP, large number of GFP-gal3 puncta (green) was observed forming after LLOMe treatment, and damaged lysosomes were unable to be cleared by autophagy after recovery. Cells with siRNA silenced negative control gene CTSC were unable to form GFP-Gal3 puncta in the LLOMe treatment (Figure 7**.**).

Original images showing GFP-Gal3 fluorescence of all 7 genes identified as potential "hits" in all three conditions (Table 4.) are further represented, and compared to the Non-target siRNA control (Figure 8. A-H). Control cells treated with 1% solvent (EtOH) show no formation of GFP-Gal 3 puncta, while LLOMe treatment showed massive number of GFP-Gal3 puncta by siRNA silencing of all the identified genes. Recovery in the FM condition showed a great increase of GFP-Gal3 puncta in all of the identified genes, compared to the Non-target control. That lead to the conclusion that these genes are required for all three pathways stated earlier. Enlarged number of GFP-Gal3 puncta in the Control-EtOH treated cells means these genes are involved in the processes of maintaining general lysosomal homeostasis. High number of puncta in the cells treated with LLOMe includes these genes in the recognition of lysosomal damage pathway. Furthermore, high number of puncta per cell in the Recovery in FM condition means these genes are also responsible for mediating the clearance and repair of those damages vesicles. All three conditions Control-EtOH, LLOMe and Recovery are represented in the columns (Figure 8.), and all of the 7 genes showed separately compared to the Non-target control siRNA images (Figure 8. H). Among the identified genes are GRTP1 (Figure 8. A), Rab3A (Figure 8. B), SYT1 (Figure 8. C), VPS11 (Figure 8. D), TBC1D3B (Figure 8. E), VPS33B (Figure 8. F), and VPS4A (Figure 8. G).

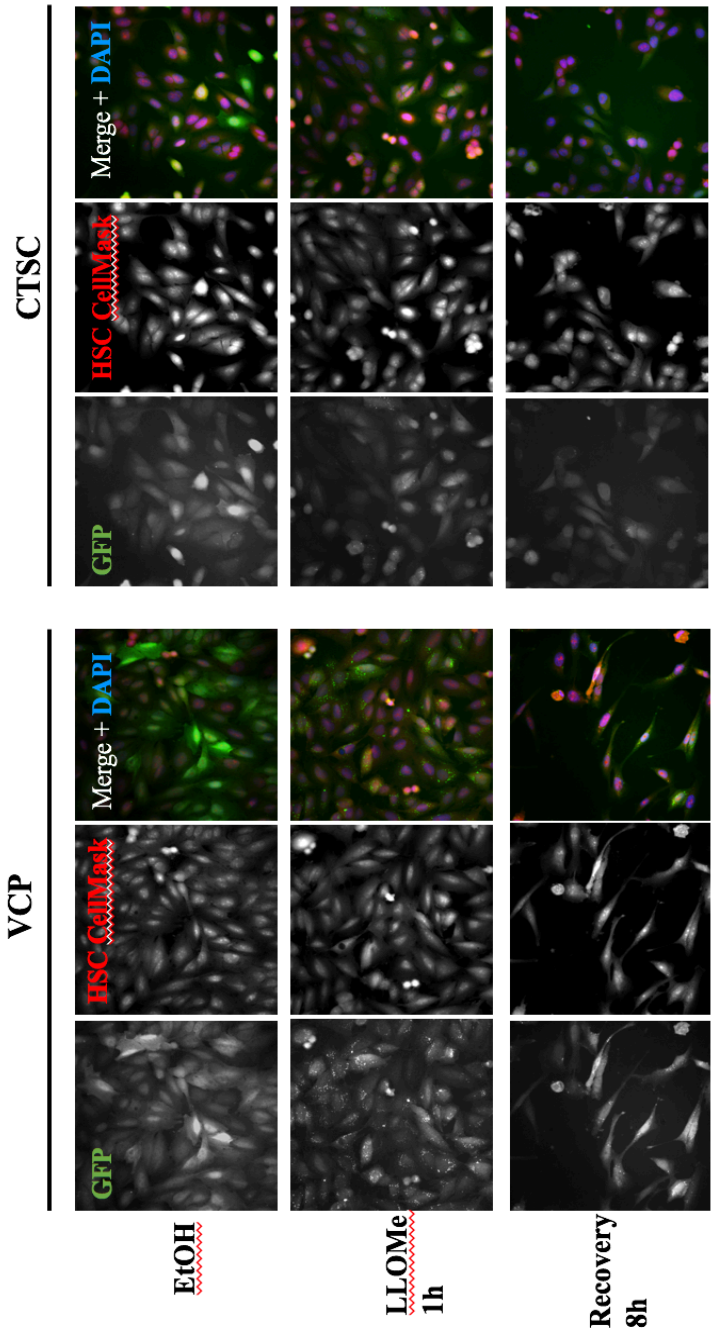

Figure 7. Original siRNA screening images of positive (VCP gene) and negative (CTSC gene) control.

VCP and CTSC genes were used as positive and negative control for the formation of LLOMe induced GFP-Gal3 puncta formation, respectively. Each condition (Control – 1% solvent, EtOH, LLOMe – 1h (1 mM), and Recovery – 8h in FM) is shown as separate channel; GFP (green), HSC CellMask (red), and a merged image with DAPI (blue).

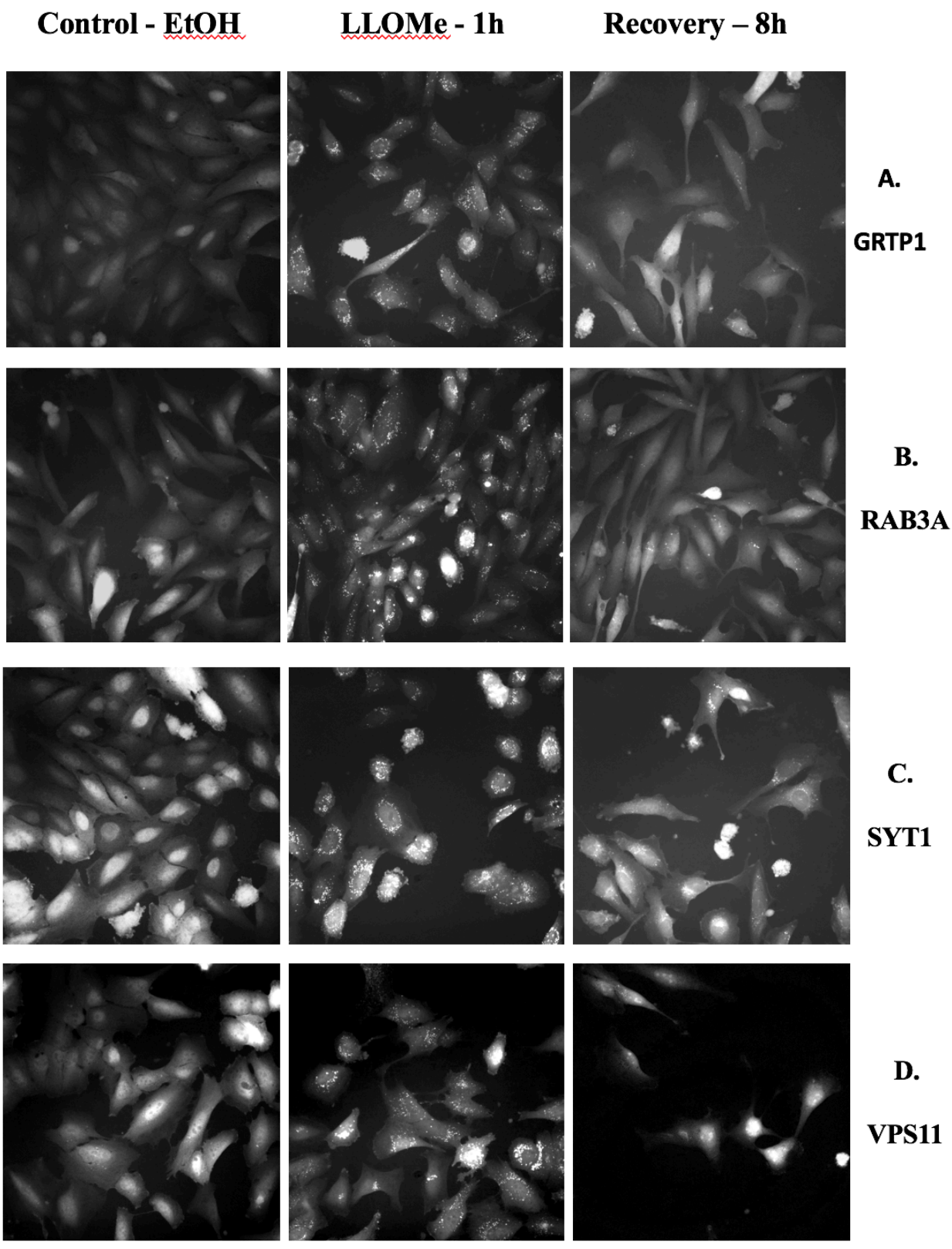
Control - EtOH
LLOMe - 1h
Recovery – 8h
A.
GRTP1
B.
RAB3A
C.
SYT1
D.
VPS11

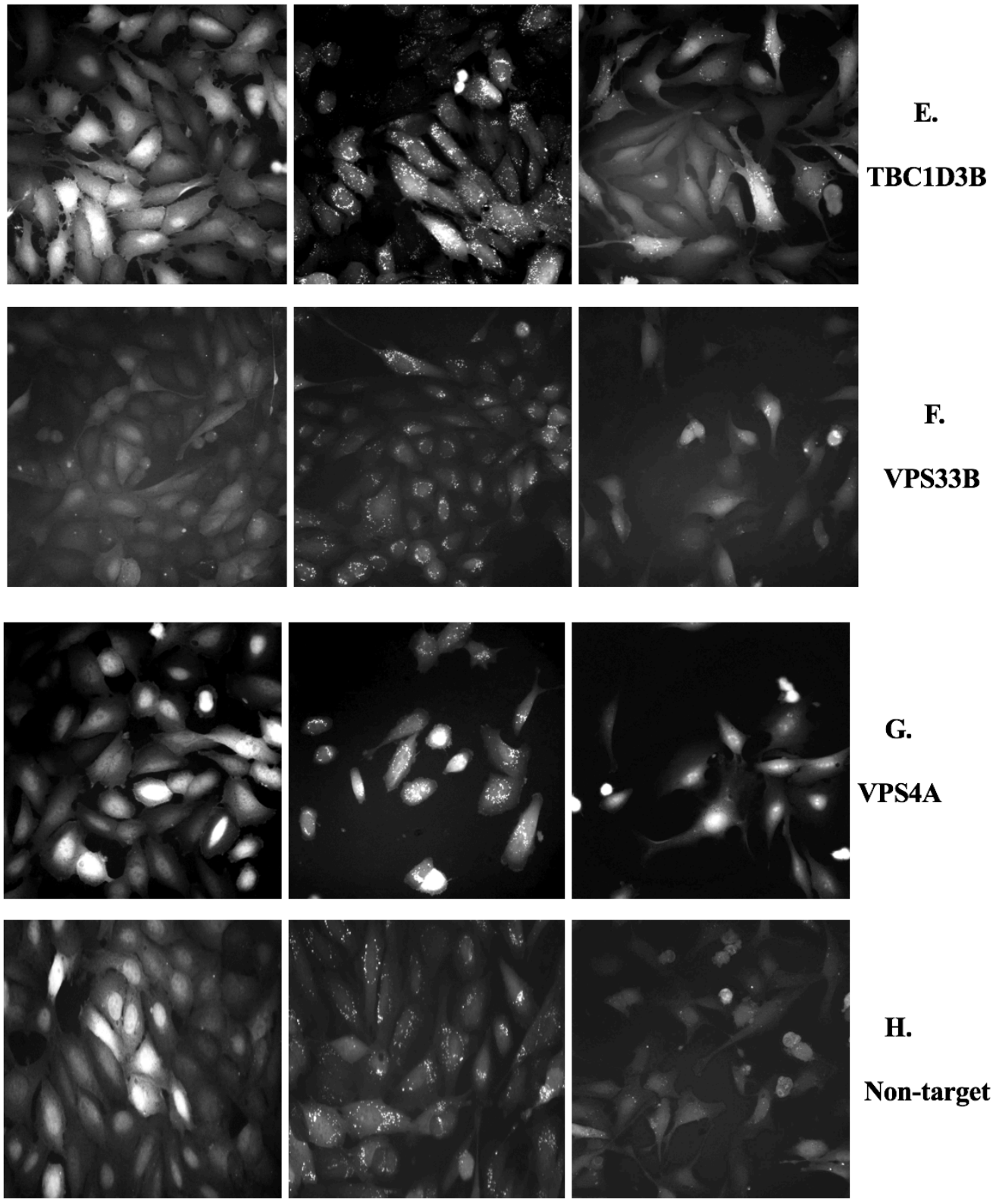

Figure 8. Original images of the 7 genes identified as possible "hits" compared to the Non-target control siRNA.
All three conditions are shown; Control – 1% solvent (EtOH), LLOMe – 1h (1 mM), and Recovery – 8h compared to the Non-target siRNA control in same conditions. Images are represented as GFP-only channel representing GFP-Gal3 in cells (shown in grayscale). A-H

images show genes GRTP1, RAB3A, SYT1, VPS11, TBC1D3B, VPS33B, VPS4A, and Non-target siRNA, respectively.

4. DISCUSSION

Model used to track lysosomal damage using GFP-Gal3 stably expressing cells was put to a test. Lysosomes ruptured by the intake of lyososomotropic agents, such as LLOMe (Maejima *et al.*, 2013), were able to be readily detected using a simple confocal microscopy. GFP tagged Galectin3 was shown to form puncta inside the cell after the initial LLOMe treatment. Observed puncta proved to be a reliable marker to track lysosomal damage co-localizing both with lysosomal membrane marker protein LAMP2, as well as autophagosome membrane marker protein LC3. Damaged lysosomes were therefore taken into the repair pathway or targeted to the autophagosomes in the process of lysophagy. Removal of the LLOMe containing media and replacing with regular Full media allowed the cells to recover and either repair or remove damaged membranes – as seen by the decrease in GFP-Gal3 puncta (after 8 hrs). Lysophagy clearance or repair of the damaged lysosomes is clearly visible by the removal of accumulated LC3 and LAMP2 markers of autophagosomes and lysosomes, respectively. When autophagy flux is impaired general markers of the pathway such as LC3 and LAMP1/2, as well as autophagy receptors such as p62 tend to accumulate in the cytosol due to the inability to be further processed into degradation, or to be recycled when the process is finished (Komatsu *et al.*, 2010).

Furthermore, the effect of LLOMe itself was tested to identify the influence lyososomotropic agents have on autophagy flux induction and progression. Using the same model cell line treated with LLOMe in one case, and left to recover in Full medium in other case, we proved via Western blot analysis that LLOMe has two-sided effect on autophagy flux. It showed to be a potent inductor of autophagy flux by stimulating the activation by phosphorylation of both ULK1 and ERK1/2 kinases responsible for early autophagosome formation. That is observed by high increase in p-ULK1 and p-ERK1/2 expression, only an hour after initial treatment with LLOMe (Moscat *et al.*, 2006; Russell, 2013). On the other hand, LLOMe proved to simultaneously inhibit the progression of autophagy flux by damaging the lysosomal membrane, and therefore final step of cargo degradation. In that case, a significant increase in LC3, GABARAP and p62 was observed, which as explained above indicates a block in autophagy progression. Since these proteins express their role in the autophagy pathway

downstream of initiation complex it is obvious to state that the block in autophagy progression happens during the autophagosome-lysosome fusion step (Pankiv, 2007). The conclusion correlates with the fact that damaged lysosomes can't be integrated into the fusion step. The defined effects of LLOMe on autophagy flux mark that specific lyosomotropic agent as a useful tool for conducting flux assays that target the middle steps of the pathway – the autophagosome maturation and closure.

Another aim of this study was to develop a strict protocol for siRNA library screening od lysosomal homeostasis genes, which was finalised and used to perform initial screening of genes involved in multiple trafficking pathways and phosphatases, the negative regulators of proteins phosphorylation pathways. During this study optimal conditions for cell maintenance, dosage and duration of treatments, and reverse transfection of siRNA conditions were recorded.

We preformed high- content screening of siRNA library using siRNAs targeting total of 486 genes. That list was separated as Membrane trafficking/G-custom genes, which included 232 genes, and Phosphatases targeting 254 genes. The former was taken into in depth statistical analysis and validation (Jung and Behrends, 2017), identifying a list of potential mediators of lysosomal biogenesis (Control – EtOH), genes involved in recognition of damaged lysosomes (LLOMe), and genes involved in clearance/repair of damaged lysosomes (Recovery). After a further validation of collected screening results 7 genes were identified from the membrane trafficking data set, to be potential novel regulators of lysosomal homeostasis, showing increased GFP-Gal3 puncta formation in all 3 conditions. Since 4 different siRNAs (pool of 4 individual siRNAs) were used to target each gene, possible off target effects binding must be considered, and each of the identified target must go through further validation, using CRISPR/Cas9 knockouts.

Out of the 7 genes RAS-Associated Protein 3A (RAB3A), member of the RAS oncogene family which consists of three other members members, Rab -3B, -3C, and -3D presents an interesting finding. The small G protein regulates Ca^{2+}-dependent neurotransmitter release, and is activated by Rab3A GDP/GTP exchange protein (Rab3A GEP) switching it from its GDP-bound inactive form to an GTP-bound active form (Tanaka *et al.*, 2001). Once activated Rab3A is found to strongly inhibit Ca^{2+}-triggered exocytosis (Schlüter *et al.*, 2002). Rab protein activity is abolished by hydrolyzation of the bound GTP to GDP mediated by its corresponding GTPase-activating protein (GAP). Furthermore, α-Synuclein, a presynaptic

protein found in Lewy bodies, a hallmark of Parkinson disease, is found to rely on the presynaptic GTPase Rab3a machinery for binding and dissociating from intracellular membranes (Chen *et al.*, 2013). More importantly, a second identified protein by this study, Growth Hormone Regulated TBC Protein 1 (GRTP1) was previously identified as Rab3A specific GAP (Ishibashi *et al.*, 2009). Third protein identified serving in the same pathway is Synaptotagmin 1 (SYT1). SYT1 is an integral membrane protein, and is thought to act as an Ca^{2+} sensor in the process of vesicular trafficking and exocytosis. Calcium binding to synaptotagmin-1 triggers neurotransmitter release at the synapse (Fernández-Chacón *et al.*, 2001). All of these three genes representing the highest scoring "hits" identified by this study, are involved in Ca^{2+} trafficking, and are found during screening for lysosomal homeostasis genes. Furthermore, they all work in the related pathway, which is found to be impaired in Parkinson's disease (Chen *et al.*, 2013). PINK1 and Parkin, known to be, when mutated, related to the familial form of Parkinson's disease (Shiba-Fukushima *et al.*, 2012), and are responsible for mitophagy occurring in cells, PINK1 acting as an receptor for damaged mitochondria (Chen and Dorn, 2013), and Parkin as an E3-ubiquitin ligase for these vesicles (Koyano *et al.*, 2014). Lysosomes themselves are known for their function in calcium storage, and are the final destination for all of the selective autophagy pathways cargo, including mitochondria.

TBC1D3B is another GTPase-activating protein identified by this study, acting on Rab5 which was found to participate in the endosomal membrane fusion reactions (Woodman, 2000). Three of the last genes found to possibly be involved in lysosomal homeostasis pathways belong to the vacuolar-protein sorting family of proteins. Vps11 and Vps33B are autophagy related genes, and part of a HOPS/CORVET complex responsible for recruitment of SNARE proteins and responsible for autophagosome-lysosome fusion (Sato *et al.*, 2000; Bach *et al.*, 2008; McEwan *et al.*, 2015). Vps4A is associated with the endosomal compartments involved in protein trafficking. It is found to co-localize with active caspases, and it is thought to regulate apoptosis via p38-MAPK pathway (Xu *et al.*, 2017). All of the genes identified by this study and listed above, considering their primary function in the cell, prove to have a logical place in the selective autophagy pathway, such as lysophagy, and consequently have a role in the lysosomal homeostasis in general.

5. CONCLUSION

In this study, we developed a model to track lysosomal membrane damage caused by the intake of lyososomotropic agent – LLOMe using a fluorophore tagged Galectin3. We identified that Galectin3 puncta form upon lysosomal damage. GFP-Galectin3 gathers from cytosolic dispersed state into localised regions marking the damaged vesicles while cells are treated with LLOMe. The puncta observed localized on both autophagosomes and lysosomes, indicating selective autophagy pathway induction.

Furthermore, we identified the effect LLOMe has on the autophagy flux being both a potent autophagy inductor, and inhibitor of autophagy progression. This knowledge works in the service of LLOMe becoming a useful tool in autophagy flux related assays.

The protocol we developed, and described in this study will be used to conduct further screening analysis involving human kinases and deubiquitinating enzymes.

High content screening of siRNA library for the genes involved in membrane trafficking and autophagy related genes ultimately presented 18 genes involved in lysosomal biogenesis (control treatment), 27 genes potentially involved in the recognition of damaged lysosomes (LLOMe treatment), and 18 genes as a possible part of the lysosome repair and/or clearance pathways (recovery treatment). 7 of these (GRTP1, RAB3A, SYT1, TBC1D3B, VPS11, VPS33B and VPS4A), involved in all three parts of lysosome homeostasis present the most valuable targets, and will be taken into further validation. They will serve to generate stable knock out cells, using the same U2OS GFP-Gal3 reporter cell line, and re-testing their influence on lysosomal biogenesis under the same conditions. That way further interaction partners, upstream and downstream effectors may be identified, and finally shape the pathways of lysosomal homeostasis. Even greater number of “hits” was observed in the screening of cell’s phosphatases, which will be further validated by statistical analysis, induvial screening of the images and eventual validation protocols, suing either single siRNA oligos or CRISPR/Cas9 knock-out cell lines.

6. SUPPLEMENTARY INFORMATION

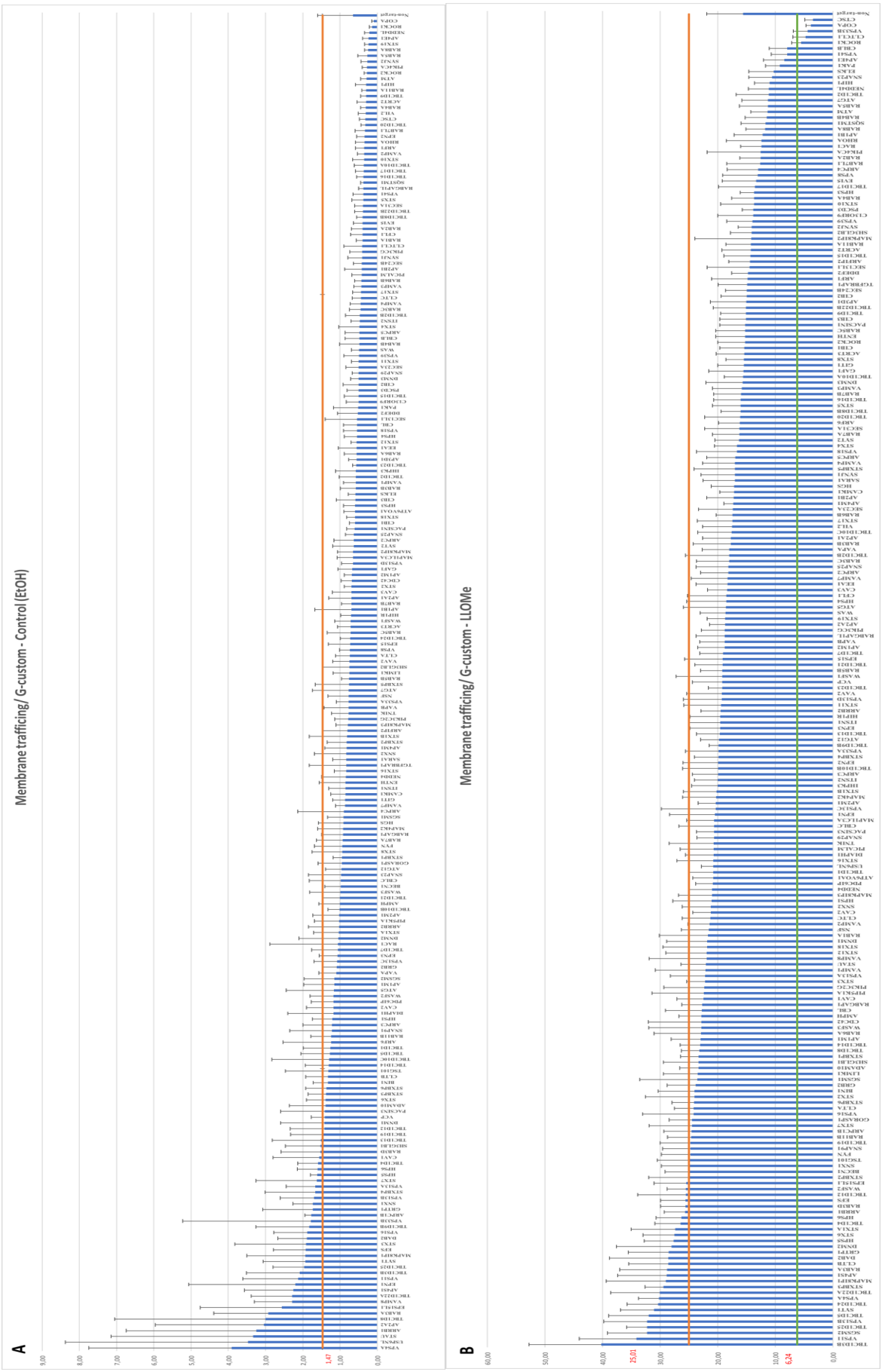

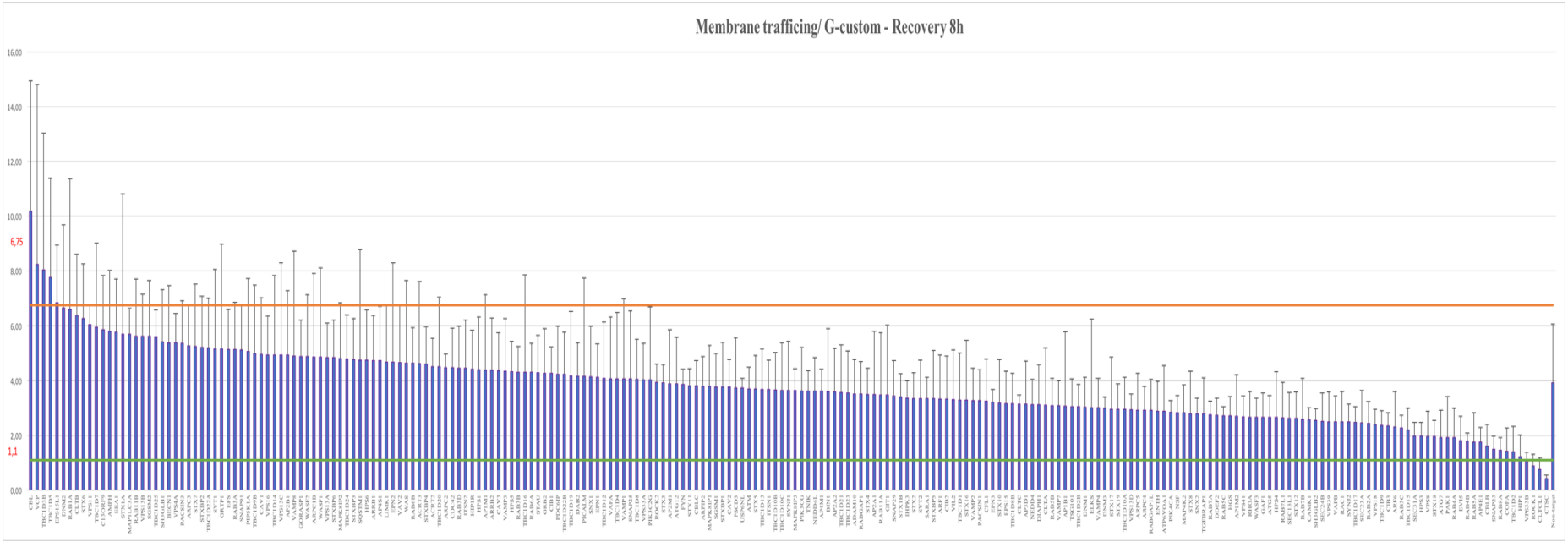
Membrane trafficing/ G-custom - Recovery 8h
16,00
14,00
12,00
10,00
6,75
8,00
6,00
4,00
2,00
1,1
0,00

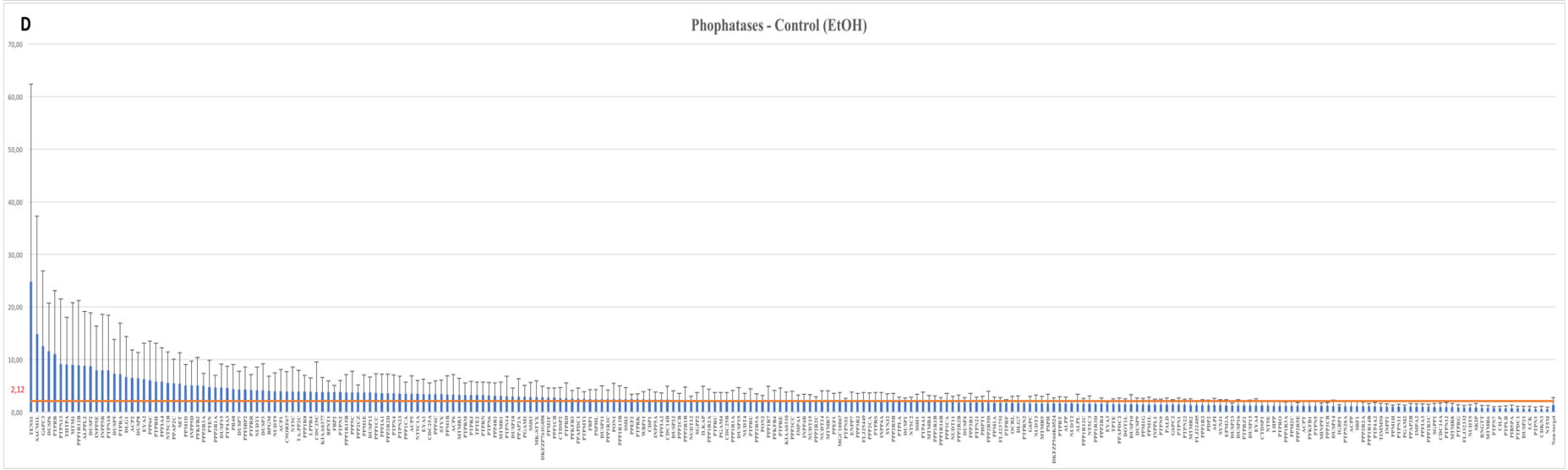
D
Phophatases - Control (EtOH)
70,00
60,00
50,00
40,00
30,00
20,00
10,00
2,12
0,00

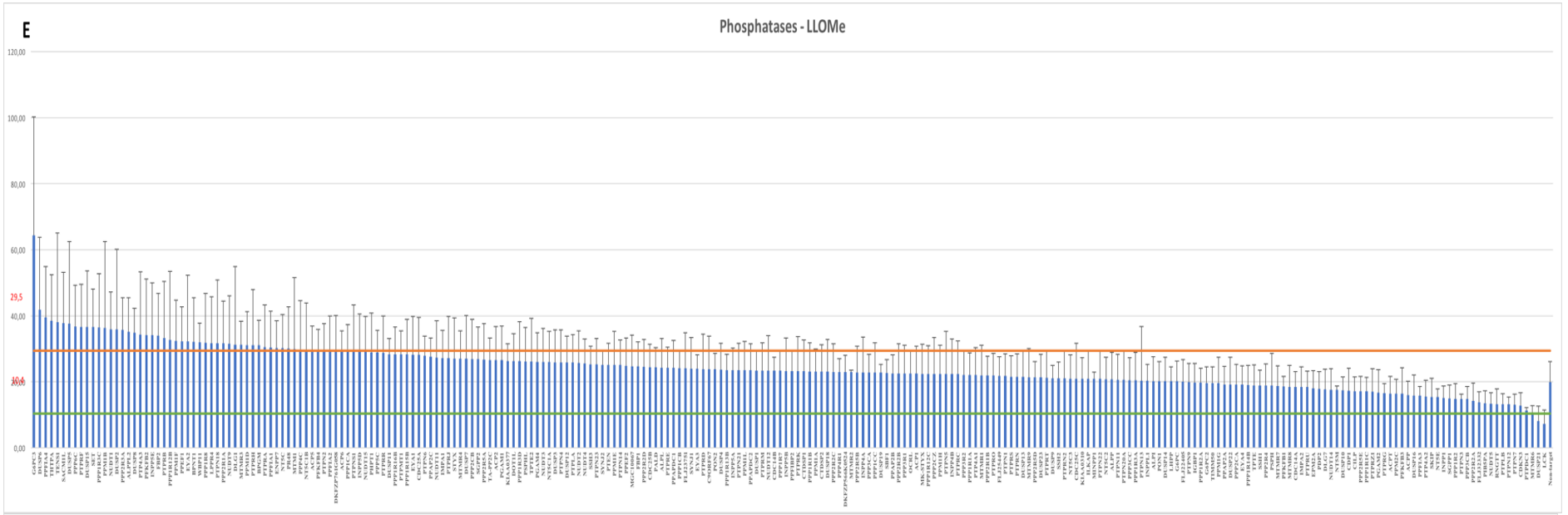
E
Phosphatases - LLOMe
120,00
100,00
80,00
60,00
29,5
40,00
20,00
0,00

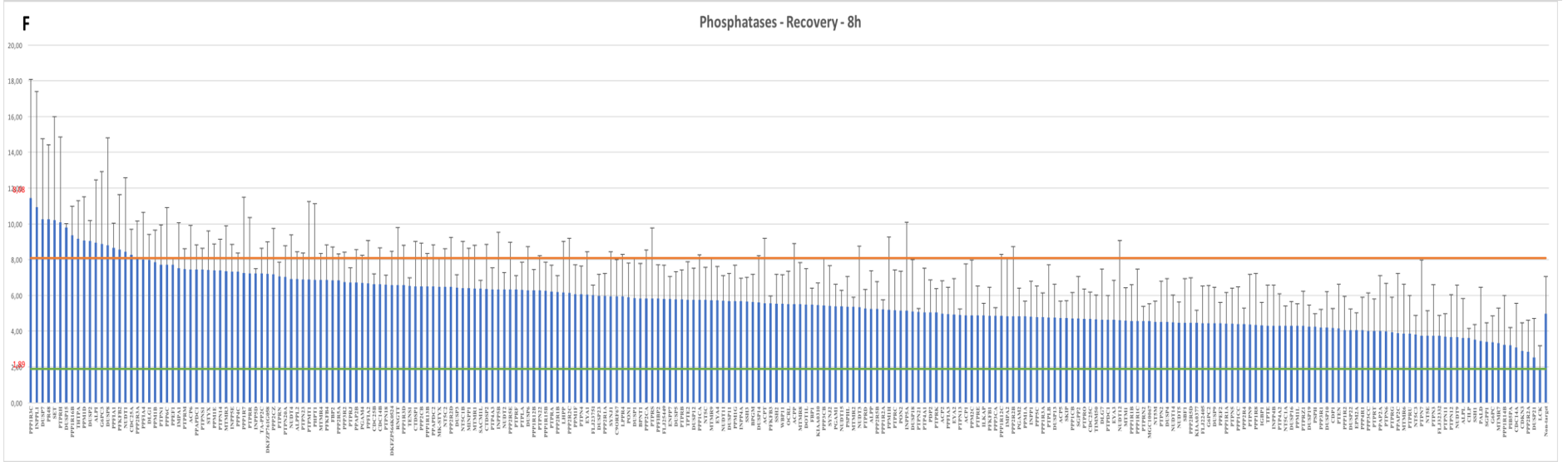
F
Phosphatases - Recovery - 8h
20,00
18,00
16,00
14,00
12,00
10,00
8,00
6,00
4,00
2,00
0,00

Image S1. sRNA screening data.
siRNA screening results represented as average puncta per cell of all the genes targeted by the used siRNA library in descending order. A-C; Membrane trafficking/custom genes separated per condition (Control – EtOH, LLOMe, Recovery respectively). Phosphatases targeted by the corresponding siRNA are presented in the same order (D-F). Calculated cut off scores are shown in red, and top and bottom cut off lines presented in orange and green respectively.

8. REFERENCES

Agarraberes, F. A., Terlecky, S. R., Dice, J. F. (1997): An intralysosomal hsp70 is required for a selective pathway of lysosomal protein degradation. *The Journal of cell biology*, **137**, 825–34.

Anding, A. L., Baehrecke, E. H. (2017): Cleaning House: Selective Autophagy of Organelles. *Developmental Cell* Elsevier Inc, **41**, 10–22.

Bach, H. *et al.* (2008): Mycobacterium tuberculosis Virulence Is Mediated by PtpA Dephosphorylation of Human Vacuolar Protein Sorting 33B. *Cell Host & Microbe*, **3**, 316–322.

Bandyopadhyay, U. *et al.* (2008): The chaperone-mediated autophagy receptor organizes in dynamic protein complexes at the lysosomal membrane. *Molecular and cellular biology* American Society for Microbiology (ASM), **28**, 5747–63.

Di Bartolomeo, S. *et al.* (2010): The dynamic interaction of AMBRA1 with the dynein motor complex regulates mammalian autophagy. *The Journal of Cell Biology*, **191**, 155–168.

Boya, P., Kroemer, G. (2008): Lysosomal membrane permeabilization in cell death. *Oncogene*, **27**, 6434–6451.

Chauhan, S. *et al.* (2016): TRIMs and Galectins Globally Cooperate and TRIM16 and Galectin-3 Co-direct Autophagy in Endomembrane Damage Homeostasis. *Developmental Cell*, **39**, 13–27.

Chen, R. H. C. *et al.* (2013): α-Synuclein membrane association is regulated by the Rab3a recycling machinery and presynaptic activity. *The Journal of biological chemistry*. **288**, 7438–49.

Chen, Y., Dorn, G.W (2013): PINK1-phosphorylated mitofusin 2 is a Parkinreceptor for culling damaged mitochondria. *Science.* **340,** 471-5.

Chen, Y., Klionsky, D. J. (2011): The regulation of autophagy - unanswered questions. *Journal of cell science*, **124**, 161–70.

Clausen, T. H. *et al.* (2010): p62/SQSTM1 and ALFY interact to facilitate the formation of p62 bodies/ALIS and their degradation by autophagy. *Autophagy*, **6**, 330–344.

Cuervo, A. M., Dice, J. F. (1996): A receptor for the selective uptake and degradation of proteins by lysosomes. *Science,* **273**, 501–3.

Dehay, B. *et al.* (2010): Pathogenic Lysosomal Depletion in Parkinson's Disease. *Journal of Neuroscience*, **30**, 12535–12544.

Deosaran, E. *et al.* (2013): NBR1 acts as an autophagy receptor for peroxisomes. *Journal of Cell Science*, **126**, 939–952.

Deter, R. L., De Duve, C. (1967): Influence of glucagon, an inducer of cellular autophagy, on some physical properties of rat liver lysosomes. *The Journal of cell biology*, **33**, 437–49.

de Duve, C., Wattiaux, R. (1966): Functions of Lysosomes. *Annual Review of Physiology*, **28**, 435–492.

Fernández-Chacón, R. *et al.* (2001): Synaptotagmin I functions as a calcium regulator of release probability. *Nature*, **410**, 41–49.

Funderburk, S. F., Wang, Q. J., Yue, Z. (2010): The Beclin 1-VPS34 complex--at the crossroads of autophagy and beyond. *Trends in cell biology*, **20**, 355–62.

Galluzzi, L. *et al.* (2017): Molecular definitions of autophagy and related processes. *The EMBO Journal*, **36**, 1811–1836.

Ganley, I. G. (2009): ULK1.ATG13.FIP200 complex mediates mTOR signaling and is essential for autophagy. *J. Biol. Chem.,* **284**, 12297–12305.

Glick, D., Barth, S., Macleod, K. F. (2010): Autophagy : cellular and molecular mechanisms. *Journal of Pathology The*, **221**, 3–12.

Gómez-Sánchez, R. *et al.* (2018): Atg9 establishes Atg2-dependent contact sites between the endoplasmic reticulum and phagophores. *The Journal of Cell Biology*, **217**, 5-15.

Grasso, D. *et al.* (2011): Zymophagy, a Novel Selective Autophagy Pathway Mediated by VMP1-USP9x-p62, Prevents Pancreatic Cell Death. *Journal of Biological Chemistry*, **286**, 8308–8324.

Gwinn, D. M. *et al.* (2008): AMPK Phosphorylation of Raptor Mediates a Metabolic Checkpoint. *Mol. Cell*, **30**, 214–226.

Hamacher-Brady, A. (2012): Autophagy Regulation and Integration with Cell Signaling. *Antioxidants & Redox Signaling*, **17**, 756–765.

Hara, K. *et al.* (2002): Raptor, a binding partner of target of rapamycin (TOR), mediates TOR action. *Cell*, **110**, 177–89.

He, C. *et al.* (2008): Self-interaction is critical for Atg9 transport and function at the phagophore assembly site during autophagy. *Molecular biology of the cell*. **19**, 5506–16.

He, Y. *et al.* (2018): p38 MAPK inhibits autophagy and promotes microglial inflammatory

responses by phosphorylating ULK1. *The Journal of Cell Biology*, **217**, 315–328.

Hornung, V. *et al.* (2008): Silica crystals and aluminum salts activate the NALP3 inflammasome through phagosomal destabilization. *Nature Immunology*, **9**, 847–856.

Ishibashi, K. *et al.* (2009): Identification and characterization of a novel Tre-2/Bub2/Cdc16 (TBC) protein that possesses Rab3A-GAP activity. *Genes to cells,* **14**, 41–52.

Jacobson, L. S. *et al.* (2013): Cathepsin-mediated Necrosis Controls the Adaptive Immune Response by Th2 (T helper type 2)-associated Adjuvants. *The Journal of Bilogical Chemistry,* **288**, 7481-7491.

Jäger, S. *et al.* (2004): Role for Rab7 in maturation of late autophagic vacuoles. *Journal of cell science*, The Company of Biologists Ltd, **117**, 4837–48.

Jiang, S., Wells, C. D., Roach, P. J. (2011): Starch-binding domain-containing protein 1 (Stbd1) and glycogen metabolism: Identification of the Atg8 family interacting motif (AIM) in Stbd1 required for interaction with GABARAPL1. *Biochemical and Biophysical Research Communications*, **413**, 420–425.

Ju, J. S. *et al.* (2009): Valosin-containing protein (VCP) is required for autophagy and is disrupted in VCP disease. *J. Cell Biol.* **217**, 875-888.

Jung, J. and Behrends, C. (2017): Protocol for Establishing a Multiplex Image-based Autophagy RNAi Screen in Cell Cultures, *BIO-PROTOCOL*, **7**(17).

Kang, H.-M. *et al.* (2018): Genome-wide identification of 99 autophagy-related (Atg) genes in the monogonont rotifer Brachionus spp. and transcriptional modulation in response to cadmium. *Aquatic Toxicology*, **201**, 73–82.

Kaushik, S. *et al.* (2008): Constitutive activation of chaperone-mediated autophagy in cells with impaired macroautophagy. *Molecular biology of the cell*, **19**, 2179–92.

Kaushik, S., Cuervo, A. M. (2009): Methods to monitor chaperone-mediated autophagy. *Methods in enzymology*, **452**, 297–324.

Kim, J. *et al.* (2011): AMPK and mTOR regulate autophagy through direct phosphorylation of ULK1. *Nat. Cell Biol,* **13**,

Kim, S. G., Buel, G. R., Blenis, J. (2013): Nutrient regulation of the mTOR complex 1 signaling pathway. *Molecules and cells*, **35**, 463–73.

Kim, S. J. *et al.* (2012): mTOR Complex 2 Regulates Proper Turnover of Insulin Receptor Substrate-1 via the Ubiquitin Ligase Subunit Fbw8. *Molecular Cell*, **48**, 875–887.

Kirkin, V. *et al.* (2009): A role for ubiquitin in selective autophagy. *Mol. Cell*, **34**, 259–269.

Klionsky, D. J. *et al.* (2003): A unified nomenclature for yeast autophagy-related genes. *Dev. Cell*, **5**, 539–545.

Köfinger, J. *et al.* (2015): Solution structure of the Atg1 complex: implications for the architecture of the phagophore assembly site. *Structure* **23**, 809–818.

Koyano, F., *et.al.* (2014): Ubiquitin is phosphorylated by PINK1 to activate Parking. *Nature,* **510,** 162-6.

Kumar, S. *et al.* (2017): Galectins and TRIMs directly interact and orchestrate autophagic response to endomembrane damage. *Autophagy*, **13**, 1086–1087.

Li, L., Chen, Y., Gibson, S. B. (2013): Starvation-induced autophagy is regulated by mitochondrial reactive oxygen species leading to AMPK activation. *Cellular Signalling*, **25**, 50–65.

Li, W. *et al.* (2018): Chaperone-mediated autophagy: Advances from bench to bedside. *Neurobiology of Disease*, In Press.

Li, W., Li, J., Bao, J. (2012): Microautophagy: lesser-known self-eating', *Cellular and Molecular Life Sciences*, **69**, 1125–1136.

Maejima, I. *et al.* (2013): Autophagy sequesters damaged lysosomes to control lysosomal biogenesis and kidney injury. *The EMBO Journal*, **32,** 2336–2347.

Maria Fimia, G. *et al.* (2007): Ambra1 regulates autophagy and development of the nervous system. *Nature*, **447**, 1121–5.

Martens, S. (2016): No ATG8s, no problem? How LC3/GAB ARAP proteins contribute to autophagy. *J. Cell Biol.* **217.**

Massey, A. C. *et al.* (2006): Consequences of the selective blockage of chaperone-mediated autophagy. *Proceedings of the Nat Acad of Sci of the USA*. **103**, 5805–10.

Mauvezin, C., Neufeld, T. P. (2015): Bafilomycin A1 disrupts autophagic flux by inhibiting both V-ATPase-dependent acidification and Ca-P60A/SERCA-dependent autophagosome-lysosome fusion. *Autophagy*, **11**, 1437–1438.

McEwan, D. G. *et al.* (2015): PLEKHM1 regulates autophagosome-lysosome fusion through HOPS complex and LC3/GABARAP proteins. *Molecular Cell*. Elsevier Inc., **57**, 39–54.

McEwan, D. G., Dikic, I. (2015): PLEKHM1: Adapting to life at the lysosome. *Autophagy*, **11**, 720-722.

McLaurin, J., Chakrabartty, A. (1996): Membrane disruption by Alzheimer beta-amyloid peptides mediated through specific binding to either phospholipids or gangliosides. Implications for neurotoxicity. *The Journal of biol. chem.*, **271**, 26482–9.

Meyer, H., Bug, M., Bremer, S. (2012): Emerging functions of the VCP/p97 AAA-ATPase in the ubiquitin system. *Nat. Cell Biol.*, **14**, 117–123.

Mijaljica, D., Prescott, M., Devenish, R. J. (2011): Microautophagy in mammalian cells:

Revisiting a 40-year-old conundrum. *Autophagy*, **7**, 673–682.

Mizushima, N. *et al.* (1998): A protein conjugation system essential for autophagy. *Nature*, **395**, 395–398

Mizushima, N. *et al.* (2008): Autophagy fights disease through cellular self-digestion. *Nature*, **451**, 1069–75.

Mizushima, N., Noda, T., Ohsumi, Y. (1999): Apg16p is required for the function of the Apg12p–Apg5p conjugate in the yeast autophagy pathway. *The EMBO Journal*, **18**, 3888–3896.

Mizushima, N., Yoshimori, T., Ohsumi, Y. (2011), The role of Atg proteins in autophagosome formation. *Annu. Rev. Cell Dev. Biol.,* **27**, 107–132.

Mochida, K. *et al.* (2015): Receptor-mediated selective autophagy degrades the endoplasmic reticulum and the nucleus. *Nature*, **522**, 359–362.

Narendra, D. *et al.* (2010): p62/SQSTM1 is required for Parkin-induced mitochondrial clustering but not mitophagy; VDAC1 is dispensable for both. *Autophagy*, **6**, 1090–1106.

Nguyen, T. N. *et al.* (2016): Atg8 family LC3/GABARAP proteins are crucial for autophagosome-lysosome fusion but not autophagosome formation during PINK1/Parkin mitophagy and starvation. *The Journal of cell biology*, **215**, 857–874.

Noda, N. N., Ohsumi, Y., Inagaki, F. (2010): Atg8-family interacting motif crucial for selective autophagy. *FEBS Lett,* **584**, 1379–1385.

Oku, M., Sakai, Y. (2018): Three Distinct Types of Microautophagy Based on Membrane Dynamics and Molecular Machineries. *BioEssays*, **40**. 180-8.

Palermo, C., Joyce, J. A. (2008): Cysteine cathepsin proteases as pharmacological targets in cancer. *Trends in Pharmacological Sciences*, **29**, 22–28.

Pankiv, S. (2007): p62/SQSTM1 binds directly to Atg8/LC3 to facilitate degradation of ubiquitinated protein aggregates by autophagy. *J. Biol. Chem.*, **282**, 24131–24145.

Paz, I. *et al.* (2010): Galectin-3, a marker for vacuole lysis by invasive pathogens. *Cellular Microbiology*, **12**, 530–544.

Pyo, J. O., Nah, J., Jung, Y. K. (2012): Molecules and their functions in autophagy. *Exp. Mol. Med.,* **44,** 73-88.

Rogov, V. V, Stolz, A., Ravichandran, A. C., Rios-Szwed, D. O., Suzuki, H., Kniss, A., Löhr, F., Wakatsuki, S., Dötsch, V., Dikic, I., Dobson, R. C., *et al.* (2017): Structural and functional analysis of the GABARAP interaction motif (GIM). *EMBO reports*, **18**, 1382–1396.

Ryu, M.-S., Duck, K. A., Philpott, C. C. (2018): Ferritin iron regulators, PCBP1 and NCOA4, respond to cellular iron status in developing red cells. *Blood Cells, Molecules, and Diseases*,

69, 75–81.

Saftig, P., Klumperman, J. (2009): Lysosome biogenesis and lysosomal membrane proteins: trafficking meets function. *Nature Reviews Molecular Cell Biology*, **10**, 623–635.

Salvador, N. *et al.* (2000): Import of a Cytosolic Protein into Lysosomes by Chaperone-Mediated Autophagy depends on its Folding State. *Journal of Biological Chemistry*, **275**, 27447–56.

Sanchez-Wandelmer, J., Reggiori, F. (2013): Amphisomes: out of the autophagosome shadow?. *The EMBO journal*, **32**, 3116–8.

Sasaki, T. *et al.* (2017): Autolysosome biogenesis and developmental senescence are regulated by both Spns1 and v-ATPase. *Autophagy*, **13**, 386–403.

Sato, T. K. *et al.* (2000): Class C Vps Protein Complex Regulates Vacuolar SNARE Pairing and Is Required for Vesicle Docking/Fusion. *Molecular Cell*, **6**, 661–671.

Schlüter, O. M. *et al.* (2002): Localization *Versus* Function of Rab3 Proteins. *Journal of Biological Chemistry*, **277**, 40919–40929.

Settembre, C. *et al.* (2013): Signals from the lysosome: a control centre for cellular clearance and energy metabolism: *Nature Reviews Molecular Cell Biology*, **14,** 283–296.

She, H. *et al.* (2018): Autophagy in inflammation: the p38α MAPK-ULK1 axis. *Immunol. Rev.,* **281**, 62-73.

Shiba-Fukushima, K., Imai, Y., Yoshida, S., Ishihama, Y., Kanao, T., Sato, S., Hattori, N. (2012): PINK1-mediatedphosphorylation of the Parkin ubiquitin-like domain primes mitoshondrial translocation of Parkin and regulates mitophagy. *Nature Sci. Reports,* **2,** 2-8.

Sorbara, M. T., Girardin, S. E. (2015): Emerging themes in bacterial autophagy. *Curr. Opin. Microbiol.* **23,** 163–170.

Stanley, R. E., Ragusa, M. J., Hurley, J. H. (2014): The beginning of the end: how scaffolds nucleate autophagosome biogenesis. *Trends in cell biology*, **24**, 73–81.

Stolz, A., Ernst, A., Dikic, I. (2014): Cargo recognition and trafficking in selective autophagy. *Nature Cell Biology*, **16**, 495–501.

Sumpter, R. *et al.* (2016): Fanconi Anemia Proteins Function in Mitophagy and Immunity. *Cell*. Elsevier, **165**, 867–81.

Suzuki, K. *et al.* (2007): Hierarchy of Atg proteins in pre-autophagosomal structure organization. *Genes to Cells*, **12**, 209–218.

Svenning, S., Johansen, T. (2013): Selective autophagy. *Essays Biochem.*, **55**, 79–92.

Tanaka, M. *et al.* (2001): Role of Rab3 GDP/GTP exchange protein in synaptic vesicle trafficking at the mouse neuromuscular junction. *Molecular biology of the cell*, **12**, 1421–30.

Thiele, D. L., Lipsky, P. E. (1990): Mechanism of L-leucyl-L-leucine methyl ester-mediated killing of cytotoxic lymphocytes: dependence on a lysosomal thiol protease, dipeptidyl peptidase I, that is enriched in these cells. *Proceedings of the Nat. Acad. of Sci. of the USA* **87**, 83–7.

Thurston, T. L. *et al.* (2012): Galectin 8 targets damaged vesicles for autophagy to defend cells against bacterial invasion. *Nature*, **482**, 414–418.

Tong, Y., Huang, H., Pan, H. (2015): Inhibition of MEK/ERK activation attenuates autophagy and potentiates pemetrexed-induced activity against HepG2 hepatocellular carcinoma cells. *Biochem. and Biophy. Research Communications*, **456**, 86–91.

Ulbricht, A. *et al.* (2015): Induction and adaptation of chaperone-assisted selective autophagy CASA in response to resistance exercise in human skeletal muscle. Autophagy, **11**, 538–546.

Villamil Giraldo, A. M. *et al.* (2014): Lysosomotropic agents: impact on lysosomal membrane permeabilization and cell death. *Biochemical Society Transactions*, **42**, 1460–1464

Wang, J. *et al.* (2009): A non-canonical MEK/ERK signaling pathway regulates autophagy via regulating Beclin 1. *The Journal of biological chem.,* **284**, 21412–24.

Wei, Y. *et al.* (2008): JNK1-Mediated Phosphorylation of Bcl-2 Regulates Starvation-Induced Autophagy. *Molecular Cell*, **30**, 678–688.

Woodman, P. G. (2000): Biogenesis of the Sorting Endosome: The Role of Rab5 Introduction – Organisation of the Endocytic Pathway. *Traffic*., **1**, 695–701.

Xu, L. *et al.* (2017): Vacuolar Protein Sorting 4B (VPS4B) Regulates Apoptosis of Chondrocytes via p38 Mitogen-Activated Protein Kinases (MAPK) in Osteoarthritis. *Inflammation*, **40**, 1924–1932.

Yamamoto, H. (2012): Atg9 vesicles are an important membrane source during early steps of autophagosome formation. *J. Cell Biol.*, **198**, 219–233.

Yoshida, Y. *et al.* (2017): Ubiquitination of exposed glycoproteins by SCF ^{FBXO27} directs damaged lysosomes for autophagy. *Proceedings of the Nat. Acad. of Sci.*, **114**, 8574–8579.

Zientara-Rytter, K., Subramani, S. (2018): AIM/LIR-based fluorescent sensors—new tools to monitor mAtg8 functions. *Autophagy*, **11**, 1–5.